Exploring Transformer Backbones for Heterogeneous Treatment Effect Estimation

Anonymous Author(s)
Affiliation
Address
email

Abstract

Neural networks (NNs) are often leveraged to represent structural similarities of potential outcomes (POs) of different treatment groups to obtain better finite-sample estimates of treatment effects. However, despite their wide use, existing works handcraft treatment-specific (sub)network architectures for representing various POs, which limit their applicability and generalizability. To remedy these issues, we develop a framework called **Trans**formers as **T**reatment **E**ffect **E**stimators (TransTEE) where attention layers govern interactions among treatments and covariates to exploit structural similarities of POs for confounding control. Using this framework, through extensive experiments, we show that TransTEE can: (1) serve as a general-purpose treatment effect estimator which significantly outperforms competitive baselines on a variety of challenging TEE problems (e.g., discrete, continuous, structured, or dosage-associated treatments.) and is applicable both when covariates are tabular and when they consist of structural data (e.g., texts, graphs); (2) yield multiple advantages: compatibility with propensity score modeling, parameter efficiency, robustness to continuous treatment value distribution shifts, interpretability in covariate adjustment, and real-world utility in debugging pre-trained language models.

1 Introduction

Recently, feed-forward neural networks have been adapted for modeling causal relationships and estimating treatment effects [34, 53, 40, 68, 8, 51, 43, 12], in part due to their flexibility in modeling nonlinear functions [28] and high-dimensional input [34]. Among them, the specialized NN's architecture plays a key role in learning representations for counterfactual inference [2, 12] such that treatment variables and covariates are well distinguished [53]. Despite these encouraging results, several key challenges make it difficult to adopt these methods as standard tools for treatment effect estimation. We argue that most current works based on subnetworks do not sufficiently exploit the structural similarities of potential outcomes for heterogeneous TEE[1] and accounting for them needs complicated regularizations, reparametrization or multi-task architectures that are problem-specific [12]. Practically, their treatment-specific designs suffer several key weaknesses, including parameter inefficiency (Table 1), brittleness under different scenarios, such as when treatments or dosages shift slightly from the training distribution (Figure 4). We discuss these problems in detail in Sections 5.1.

To overcome the above challenges and motivated by the observation that model structure plays a crucial role in TEE [2, 12], we provide compelling evidence that transformers can outperform multilayer perceptrons and offer a promising alternative approach when leveraging deep learning to estimate treatment effects. Our work bulds on the Transformer architecture [60] which has emerged as an architecture of choice for diverse domains, including natural language processing [60], image recognition [17], and multimodal processing [57].

[1]For example, $\mathbb{E}[Y(1) - Y(0)|X]$ is often of a much simpler form to estimate than either $\mathbb{E}[Y(1)|X]$ or $\mathbb{E}[Y(0)|X]$, due to inherent similarities between $Y(1)$ and $Y(0)$.

Submitted to 36th Conference on Neural Information Processing Systems (NeurIPS 2022). Do not distribute.

Table 1: **Comparison of existing works and TransTEE in terms of parameter complexity.** n is the number of treatments. B_T, B_D are the number of branches for approximating continuous treatment and dosage. Treatment interaction means explicitly modeling collective effects of multiple treatments. TransTEE is general for all the factors.

METHODS	DISCRETE TREATMENT	CONTINUOUS TREATMENT	TREATMENT INTERACTION	DOSAGE
TARNET [53]	$\mathcal{O}(n)$			
PERFECT MATCH [52]	$\mathcal{O}(n)$		$\mathcal{O}(2^T)$	
DRAGONNET [54]	$\mathcal{O}(n)$			
DRNET [51]	$\mathcal{O}(n)$			$\mathcal{O}(TB_D)$
SCIGAN [8]	$\mathcal{O}(n)$			$\mathcal{O}(TB_D)$
VCNET [43]	$\mathcal{O}(1)$	$\mathcal{O}(1)$		
NCORE [44]	$\mathcal{O}(n)$	$\mathcal{O}(B_T)$	$\mathcal{O}(n)$	
FLEXTENET [12]	$\mathcal{O}(n)$			
OURS	$\mathcal{O}(1)$	$\mathcal{O}(1)$	$\mathcal{O}(1)$	$\mathcal{O}(1)$

In this paper, we investigate the following question: *can Transformers be similarly effective for treatment effect estimation in problems of practical interest?* Throughout, we adopt the notation of the Rubin-Neyman potential outcomes framework [47] and focus on conditional average treatment effect (CATE) estimation. In particular, we develop TransTEE, a method that builds upon the attention mechanisms and achieves state-of-the-art on a wide range of TEE tasks. Note that Transformer is originally designed for sequence modeling, to utilize its power in TEE, three key design choices are proposed. First, *treatment and covariate embedding layer* is used to represent covariate and treatment variables separately via learnable embeddings. This design is parameter-efficient in comparison to related works and we show that it appears to perform better under some practically-motivated treatment shifts.

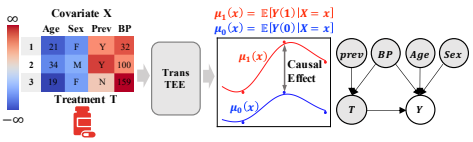

Figure 1: **A motivating example** with a corresponding causal graph. **Prev** denotes previous infection condition and **BP** denotes blood pressure. TransTEE adjusts an appropriate covariate set $\{\textbf{Prev}, \textbf{BP}\}$ with attention which is visualized via a heatmap.

In summary, we make the following contributions:

- We propose TransTEE to explore the design space of TEE, showing that Transformers, equipped with the proposed design choices, can be effective and versatile treatment effect estimators under the Rubin-Neyman potential outcomes framework. TransTEE is empirically verified to be (i) a general framework applicable for a wide range of neural TEE settings; (ii) compatible with propensity score modeling; (ii) parameter-efficient; (ii) robust under treatment shifts; (iv) interpretable in covariate adjustment; (v) deliverable for real-world utility beyond semi-synthetic settings.
- Experiments on six benchmarks with four types of treatments are conducted under various scenarios to verify the effectiveness of TransTEE and propensity score regularized adversarial training in estimating treatment effects. We show that TransTEE produces covariate adjustment interpretation and significant performance gains given discrete, continuous or structured treatments on popular benchmarks including IHDP, News, TCGA. An empirical study on pre-trained language models is conducted to show the real-world utility of TransTEE that implies potential applications.

2 Related Work

Neural Treatment Effect Estimation. There are many recent works on adapting neural networks to learn counterfactual representations for treatment effect estimation [34, 53, 40, 68, 8, 51, 43, 12]. To mitigate the imbalance of covariate representations across treatment groups, various approaches are proposed including optimizing distributional divergence (e.g. IPM including MMD, Wasserstein distance), entropy balancing [69] (converges to JSD between groups), counterfactual variance [71].

3 Problem Statement and Assumptions

Treatment Effect Estimation. We consider a setting in which we are given N observed samples $(\mathbf{x}_i, t_i, s_i, y_i)_{i=1}^N$, each containing N pre-treatment covariates $\{\mathbf{x}_i \in \mathbb{R}^p\}_{i=1}^N$. The treatment variable t_i in this work has various support, e.g., $\{0, 1\}$ for binary treatment settings, $\mathbb{R}$ for continuous

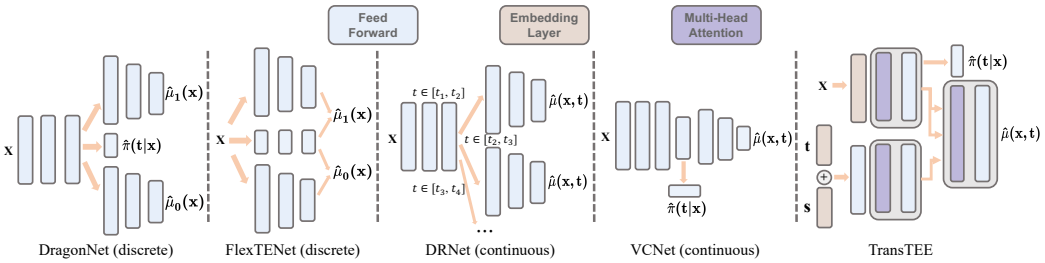

Figure 2: **A schematic comparison** of TransTEE and recent works including DragonNet[54], FlexTENet[12], DRNet[51] and VCNet[43]. TransTEE handles all the scenarios without handcrafting treatment-specific architectures and any additional parameter overhead.

treatment settings, and graphs/words for structured treatment settings. For each sample, the potential outcome (μ-model) $\mu(\mathbf{x}, t)$ or $\mu(\mathbf{x}, t, s)$ is the response of the i-th sample to a treatment t, where in some cases each treatment will be associated with a dosage $s_{t_i} \in \mathbb{R}$. The propensity score (π-model) is the conditional probability of treatment assignment given the observed covariates $\pi(T = t|X = \mathbf{x})$. The above two models can be parameterized as μ_θ and π_ϕ, respectively. The task is to estimate the Average Dose Response Function (ADRF): $\mu(\mathbf{x}, t) = \mathbb{E}[Y|X = \mathbf{x}, do(T = t)]$ [55], which includes special cases in discrete treatment scenarios that can also be estimated as the average treatment effect (ATE): $ATE = \mathbb{E}[\mu(\mathbf{x}, 1) - \mu(\mathbf{x}, 0)]$ and its individual version ITE.

Assumption 3.1. (Ignorability/Unconfoundedness) implies no hidden confounders such that $Y(T = t) \perp\!\!\!\perp T|X$. In the binary treatment case, $Y(0), Y(1) \perp\!\!\!\perp T|X$.

Assumption 3.2. (Positivity/Overlap) The treatment assignment is non-deterministic such that, i.e. $0 < \pi(t|x) < 1, \forall x \in \mathcal{X}, t \in \mathcal{T}$

4 TransTEE: Transformers as Treatment Effect Estimators

Preliminary. The main module in TransTEE is the attention layer [60]: given d-dimensional query, key, and value matrices $Q \in \mathbb{R}^{d \times d_k}, K \in \mathbb{R}^{d \times d_k}, V \in \mathbb{R}^{d \times d_v}$, attention mechanism computes the outputs as $\mathcal{H}(Q, K, V) = \text{softmax}(\frac{QK^T}{\sqrt{d_k}})V$. In practice, multi-head attention is preferable to jointly attend to the information from different representation subspaces at different positions.

$$\mathcal{H}_M(Q, K, V) = \text{Concat}(head_1, ..., head_h)W^O, \text{where } head_i = \mathcal{H}(QW_i^Q, KW_i^K, VW_i^V),$$

where $W_i^Q \in \mathbb{R}^{d \times d_k}, W_i^V \in \mathbb{R}^{d \times d_k}, W_i^V \in \mathbb{R}^{d \times d_v}$ and $W^O \in \mathbb{R}^{hd_v \times d}$ are learnable matrices.

4.1 Covariate and Treatment Embedding Layers

Treatment Embedding Layer. As illustrated in Figure 2 and Table. 1, as treatments are often of much lower dimension compared to covariates, to avoid missing the impacts of treatments, previous works (e.g., DragonNet [54], FlexTENet [12], DRNet [51]) assign covariates from different treatment groups to different branches, which is *highly parameter inefficient*. Besides, We analyze in Proposition 2 (Appendix D) that, for continuous treatments/dosages, the performance is affected by both number of branches and the value interval of treatment. However, almost all previous works on continuous treatment/dosage assume the treatment or dosage is in a fixed value interval e.g., $[0, 1]$ and Figure 4 shows that prevalent works *fail when tested under shifts of treatments*. These two observations motivate us to use two learnable linear layers to project scalar treatments and dosages to d-dimension vectors separately:

$$M_t = \text{Linear}(t), M_s = \text{Linear}(s),$$

where $M_t \in \mathbb{R}^d$. $M_s \in \mathbb{R}^d$ exists just when each treatment has a dosage parameter, otherwise only treatment embedding is needed. When multiple (n) treatments act simultaneously, the projected matrix will be $M_t \in \mathbb{R}^{d \times n}, M_s \in \mathbb{R}^{d \times n}$ and when facing structural treatments (languages, graphs), the treatment embedding will be projected by language models and graph neural networks respectively. By using the treatment embeddings, TransTEE is shown to be (i) *robust under treatment shifts*, and (ii) *parameter-efficient*.

Covariates Embedding Layer. Different from previous works that embed all covariates by one fully connected layer, where the differences between covariate tend to be lost, and is hard to study

the function of an individual covariate in a sample. TransTEE learns different embeddings for each covariate, namely $M_x = \text{Linear}(\mathbf{x})$, and $M_x \in \mathbb{R}^{d\times p}$, where p is the number of covariate. Covariates embedding enables us to study the effect of individual covariate on the outcome.

4.2 Covariate and Treatment Self-Attention

For covariates, prevalent methods represent covariates as a whole feature using MLPs, where pairwise covariate interactions are lost when adjusting covariates. Therefore, we cannot study the effect of each covariate on the estimated result. In contrast, TransTEE processes each covariate embedding independently and model their interactions by self-attention layers. Namely,

$$\hat{M}_x^l = \mathcal{H}_M(M_x^{l-1}, M_x^{l-1}, M_x^{l-1}) + M_x^{l-1}, M_x^l = \text{MLP}(\text{BN}(\hat{M}_x^l)) + \hat{M}_x^l.$$

where M_x^l is the output of l layer and BN is the BatchNorm layer. Simultaneously, the treatments and dosages embeddings are concatenated and projected to the latent dimension by a linear layer, which generates a new embedding $M_{st} \in \mathbb{R}^d$. Then self-attention is applied

$$M_{st}^l = \mathcal{H}_M(M_{st}^{l-1}, M_{st}^{l-1}, M_{st}^{l-1}) + M_{st}^{l-1}, M_{st}^l = \text{MLP}(\text{BN}(\hat{M}_{st}^l)) + \hat{M}_{st}^l.$$

The self-attention layer for treatments enables treatment interactions, an important desideratum for S- and T-learners. Namely, TransTEE can *model the scenario where multiple treatments are applied and attains strong practical utility*, e.g., multiple prescriptions in healthcare or different financial measures in economics. This is an effective remedy for existing methods which are limited to settings where various treatments are not used simultaneously.

4.3 Treatment-Covariate Cross-Attention

One of the fundamental challenges of causal meta-learners is to model treatment-covariate interactions. TransTEE realizes such a goal by a cross-attention module, treating M_{st} as query and M_x as both key and value

$$\begin{aligned}
\hat{M}^l &= \mathcal{H}_M(M_{st}^{l-1}, M_x^{l-1}, M_x^{l-1}) + M^{l-1}, \\
M^l &= \text{MLP}(\hat{M}^l) + \hat{M}^l, \\
\hat{y} &= \text{MLP}(\text{Pooling}(M^L)),
\end{aligned}$$

where M^L is the output of the last cross-attention layer and $M^0 = M_{st}^L$. The above interactions are particularly important for adjusting proper covariate or confounder sets for estimating treatment effects [59], which empirically yields *suitable covariate adjustment principles (the Disjunctive Cause Criteria) [14, 59] about pre-treatment covariates and confounders* as intuitively illustrated in Figure 1 and corroborated in our experiments.

Denote $\hat{y} \coloneqq \mu_\theta(\mathbf{x}, t)$ and the training objective is the mean square error (MSE) of the outcome regression is

$$\mathcal{L}_\theta(\mathbf{x}, y, t) = \sum_{i=1}^{n} \left(y_i - \mu_\theta(\mathbf{x}_i, t_i)\right)^2. \tag{1}$$

In summary, thanks to the designs described above for modeling treatments and covariates, when combined with strong modeling capacity of Transformers, *TransTEE can be extended to high-dimensional data easily and effectively* on tabular, graph, textual data. The generalizability of the TransTEE also allows new applications like auditing language models beyond semi-synthetic settings as shown in the next section. We include an illustration of the TransTEE workflow using a concrete example in Appendix B.

5 Experimental Results

We elaborate basic experimental settings, results, analysis and empirical studies in this section. See Appendix E for full details of all experimental settings and detailed definition of metrics. See Appendix F for many more results and remarks.

5.1 Case Study and Numerical Results

Case study on treatment distribution shifts We start by conducting a case study on treatment distribution shifts (Figure 4), and exploring an extrapolation setting in which the treatment may

Table 2: **Experimental results comparing NN based methods on the IHDP datasets,** where —— means the model is not suitable for continuous treatments. We report the results based on 100 repeats, and numbers after $\pm$ are the estimated standard deviation of the average value. For the vanilla setting with binary treatment, we report the mean absolute difference between the estimated and true ATE. For Extrapolation ($h = 2$), models are trained with $t \in [0.1, 2.0]$ and tested in $t \in [0, 2.0]$. For Extrapolation ($h = 5$), models are trained with $t \in [0.25, 5.0]$ and tested in $t \in [0, 5]$.

METHODS	VANILLA (BINARY)	VANILLA ($h = 1$)	EXTRAPOLATION ($h = 2$)	VANILLA ($h = 5$)	EXTRAPOLATION ($h = 5$)
TARNET	0.3670 ± 0.61112	2.0152 ± 1.07449	12.967 ± 1.78108	5.6752 ± 0.53161	31.523 ± 1.5013
DRNET	0.3543 ± 0.60622	2.1549 ± 1.04483	11.071 ± 0.99384	3.2779 ± 0.42797	31.524 ± 1.50264
FLEXTENET	0.2700 ± 0.10000	——	——	——	——
VCNET	0.2098 ± 0.18236	0.7800 ± 0.61483	NAN	NAN	NAN
TRANSTEE	$\mathbf{0.0983 \pm 0.15384}$	0.1151 ± 0.10289	0.2745 ± 0.14976	0.1621 ± 0.14443	0.2066 ± 0.23258
TRANSTEE+MLE	0.1721 ± 0.40061	0.0877 ± 0.03352	0.2685 ± 0.17552	0.2079 ± 0.17637	0.1476 ± 0.07123
TRANSTEE+TR	0.1913 ± 0.29953	0.0781 ± 0.03243	0.2393 ± 0.08154	$\mathbf{0.1143 \pm 0.03224}$	$\mathbf{0.0947 \pm 0.0824}$
TRANSTEE+PTR	0.2193 ± 0.34667	$\mathbf{0.0762 \pm 0.07915}$	$\mathbf{0.2352 \pm 0.17095}$	0.1363 ± 0.08036	0.1363 ± 0.08035

subsequently be administered at values never seen before during training. Surprisingly, we find that while standard results rely constraining the values of treatments [43] and dosages [51] to a specific range, our methods perform surprisingly well when extrapolating beyond these ranges as assessed on several empirical benchmarks. By comparison, many other methods appear comparatively brittle on these same settings. See Appendix D for detailed discussion and analysis.

Case study of propensity modeling. TransTEE is conceptually simple and effective. However, when the sample size is small, it becomes important to account for selection bias [2]. However, most existing regularizations can only be used when the treatments are discrete [7, 37, 18]. Thus we propose two regularization variants for continuous treatment/dosages, which are termed Treatment Regularization (TR, $\mathcal{L}_\phi^{TR}(\mathbf{x}, t) = \sum_{i=1}^n \left(t_i - \pi_\phi(\hat{t}_i|\mathbf{x}_i)\right)^2$) and its probabilistic version Probabilistic Treatment Regularization (PTR, $\mathcal{L}_\phi^{PTR} = \sum_{i=1}^n \left[\frac{(t_i - \pi_\phi(\mu|\mathbf{x}_i))^2}{2\pi_\phi(\sigma^2|\mathbf{x}_i)} + \frac{1}{2}\log \pi_\phi(\sigma^2|\mathbf{x}_i)\right]$) respectively. The overall model is trained in a adversarial pattern, namely $\min_\theta \max_\phi \mathcal{L}_\theta(\mathbf{x}, y, t) - \mathcal{L}_\phi(\mathbf{x}, t)$. Specifically, a propensity score model $\pi_\phi(t|\mathbf{x})$ parameterized by an MLP is learned by minimizing $\mathcal{L}_\phi(\mathbf{x}, t)$, and then the outcome estimators $\mu_\theta(\mathbf{x}, t)$ is trained by $\min_\theta \mathcal{L}_\theta(\mathbf{x}, y, t) - \mathcal{L}_\phi(\mathbf{x}, t)$. To overcome selection biases over representation space, the bilevel optimization enforces effective treatment effect estimation while modeling the discriminative propensity features to partial out parts of covariates that cause the treatment but not the outcome and dispose of nuisance variations of covariates [36].

Continuous dosage. In Table 3, we compare TransTEE against baselines on the TCGA (D) dataset with default treatment selection bias 2.0 and dosage selection bias 2.0. As the number of treatments increases, TransTEE and its variants (with regularization term) consistently outperform the baselines by a large margin on both training and test data. TransTEE's effectiveness is also shown in Appendix Figure 6, where the estimated ADRF curve of each treatment considering continuous dosages is plotted. Compared to baselines, TransTEE attains better results over all treatments. Stronger selection bias in the observed data makes estimation more difficult because it becomes less likely to see certain treatments or particular covariates. Considering different dosage and treatment selection bias, Appendix Figure 5 shows that as biases increase, TransTEE consistently performs the best.

Structured treatments. We compared the performance of TransTEE to baselines on the training and test set of both SW and TCGA datasets with varying degrees of treatment selection bias. The numerical results are shown in Appendix Table 9. The performance gain between GNN and Zero indicates that taking into account of graph information significantly improves estimation. The results suggest that, overall, the performance of TransTEE is the best due to the strong modeling capability and advanced model structure for processing high-dimensional treatments. SIN is the best model among these baselines.

6 Concluding Remarks

In this work, we show that transformers can be effective and versatile treatment effect estimators. Extensive experiments well verify the effectiveness and utility of TransTEE, which also imply that a more challenging and unified evaluation alternatives of TEE with domain experts are needed.

References

[1] Alberto Abadie and Guido W Imbens. Matching on the estimated propensity score. *Econometrica*, 2016.

[2] Ahmed Alaa and Mihaela Schaar. Limits of estimating heterogeneous treatment effects: Guidelines for practical algorithm design. In *ICML*, 2018.

[3] Ahmed M Alaa and Mihaela van der Schaar. Bayesian inference of individualized treatment effects using multi-task gaussian processes. In *NeurIPS*, 2017.

[4] Ahmed M Alaa, Michael Weisz, and Mihaela Van Der Schaar. Deep counterfactual networks with propensity-dropout. *arXiv*, 2017.

[5] Peter C Austin. An introduction to propensity score methods for reducing the effects of confounding in observational studies. *Multivariate behavioral research*, 2011.

[6] Shai Ben-David, John Blitzer, Koby Crammer, Alex Kulesza, Fernando Pereira, and Jennifer Wortman Vaughan. A theory of learning from different domains. *Machine learning*, 2010.

[7] Ioana Bica, Ahmed M Alaa, James Jordon, and Mihaela van der Schaar. Estimating counterfactual treatment outcomes over time through adversarially balanced representations. *arXiv*, 2020.

[8] Ioana Bica, James Jordon, and Mihaela van der Schaar. Estimating the effects of continuous-valued interventions using generative adversarial networks. 2020.

[9] Kyle Chang, Chad J Creighton, Caleb Davis, Lawrence Donehower, Jennifer Drummond, David Wheeler, Adrian Ally, Miruna Balasundaram, Inanc Birol, Yaron SN Butterfield, et al. The cancer genome atlas pan-cancer analysis project. *Nat Genet*, 2013.

[10] Mark Chen, Jerry Tworek, Heewoo Jun, Qiming Yuan, Henrique Ponde de Oliveira Pinto, Jared Kaplan, Harri Edwards, Yuri Burda, Nicholas Joseph, Greg Brockman, et al. Evaluating large language models trained on code. *arXiv*, 2021.

[11] Jonathan Crabbé, Alicia Curth, Ioana Bica, and Mihaela van der Schaar. Benchmarking heterogeneous treatment effect models through the lens of interpretability. *arXiv preprint arXiv:2206.08363*, 2022.

[12] Alicia Curth and Mihaela van der Schaar. On inductive biases for heterogeneous treatment effect estimation. In *NeurIPS*, 2021.

[13] Ralph B D'Agostino. Propensity score methods for bias reduction in the comparison of a treatment to a non-randomized control group. *Statistics in medicine*, 1998.

[14] Xavier De Luna, Ingeborg Waernbaum, and Thomas S Richardson. Covariate selection for the nonparametric estimation of an average treatment effect. *Biometrika*, 2011.

[15] Peng Ding, TJ VanderWeele, and James M Robins. Instrumental variables as bias amplifiers with general outcome and confounding. *Biometrika*, 2017.

[16] Alexey Dosovitskiy, Lucas Beyer, Alexander Kolesnikov, Dirk Weissenborn, Xiaohua Zhai, Thomas Unterthiner, Mostafa Dehghani, Matthias Minderer, Georg Heigold, Sylvain Gelly, et al. An image is worth 16x16 words: Transformers for image recognition at scale. 2021.

[17] Alexey Dosovitskiy, Lucas Beyer, Alexander Kolesnikov, Dirk Weissenborn, Xiaohua Zhai, Thomas Unterthiner, Mostafa Dehghani, Matthias Minderer, Georg Heigold, Sylvain Gelly, Jakob Uszkoreit, and Neil Houlsby. An image is worth 16x16 words: Transformers for image recognition at scale. In *ICLR*, 2021.

[18] Xin Du, Lei Sun, Wouter Duivesteijn, Alexander Nikolaev, and Mykola Pechenizkiy. Adversarial balancing-based representation learning for causal effect inference with observational data. *DMKD*, 2021.

[19] Amir Feder, Nadav Oved, Uri Shalit, and Roi Reichart. Causalm: Causal model explanation through counterfactual language models. *Computational Linguistics*, 2021.

[20] Constantine E Frangakis and Donald B Rubin. Principal stratification in causal inference. *Biometrics*, 2002.

[21] Michele Jonsson Funk, Daniel Westreich, Chris Wiesen, Til Stürmer, M Alan Brookhart, and Marie Davidian. Doubly robust estimation of causal effects. *American journal of epidemiology*, 2011.

[22] Yaroslav Ganin, Evgeniya Ustinova, Hana Ajakan, Pascal Germain, Hugo Larochelle, François Laviolette, Mario Marchand, and Victor Lempitsky. Domain-adversarial training of neural networks. *JMLR*, 2016.

[23] Matt Gardner, Yoav Artzi, Victoria Basmov, Jonathan Berant, Ben Bogin, Sihao Chen, Pradeep Dasigi, Dheeru Dua, Yanai Elazar, Ananth Gottumukkala, et al. Evaluating models' local decision boundaries via contrast sets. In *EMNLP Findings*, 2020.

[24] Zhenyu Guo, Shuai Zheng, Zhizhe Liu, Kun Yan, and Zhenfeng Zhu. Cetransformer: Casual effect estimation via transformer based representation learning. In *PRCV*, 2021.

[25] Shonosuke Harada and Hisashi Kashima. Graphite: Estimating individual effects of graph-structured treatments. In *CIKM*, 2021.

[26] Jennifer L Hill. Bayesian nonparametric modeling for causal inference. *Journal of Computational and Graphical Statistics*, 2011.

[27] Keisuke Hirano, Guido W Imbens, and Geert Ridder. Efficient estimation of average treatment effects using the estimated propensity score. *Econometrica*, 2003.

[28] Kurt Hornik, Maxwell Stinchcombe, and Halbert White. Multilayer feedforward networks are universal approximators. *Neural networks*, 1989.

[29] Andrew Ilyas, Sung Min Park, Logan Engstrom, Guillaume Leclerc, and Aleksander Madry. Datamodels: Predicting predictions from training data. *arXiv*, 2022.

[30] Guido W Imbens and Donald B Rubin. *Causal inference in statistics, social, and biomedical sciences*. Cambridge University Press, 2015.

[31] Alon Jacovi and Yoav Goldberg. Towards faithfully interpretable nlp systems: How should we define and evaluate faithfulness? *arXiv preprint arXiv:2004.03685*, 2020.

[32] Andrew Jaegle, Sebastian Borgeaud, Jean-Baptiste Alayrac, Carl Doersch, Catalin Ionescu, David Ding, Skanda Koppula, Daniel Zoran, Andrew Brock, Evan Shelhamer, Olivier J Henaff, Matthew Botvinick, Andrew Zisserman, Oriol Vinyals, and Joao Carreira. Perceiver IO: A general architecture for structured inputs & outputs. In *ICLR*, 2022.

[33] Andrew Jaegle, Felix Gimeno, Andy Brock, Oriol Vinyals, Andrew Zisserman, and Joao Carreira. Perceiver: General perception with iterative attention. In *ICML*, 2021.

[34] Fredrik Johansson, Uri Shalit, and David Sontag. Learning representations for counterfactual inference. In *ICML*, 2016.

[35] Fredrik D Johansson, Uri Shalit, Nathan Kallus, and David Sontag. Generalization bounds and representation learning for estimation of potential outcomes and causal effects. *arXiv*, 2020.

[36] Jean Kaddour, Yuchen Zhu, Qi Liu, Matt J Kusner, and Ricardo Silva. Causal effect inference for structured treatments. 2021.

[37] Nathan Kallus. Deepmatch: Balancing deep covariate representations for causal inference using adversarial training. In *ICML*, 2020.

[38] Joseph DY Kang and Joseph L Schafer. Demystifying double robustness: A comparison of alternative strategies for estimating a population mean from incomplete data. *Statistical science*, 2007.

[39] Jacob Devlin Ming-Wei Chang Kenton and Lee Kristina Toutanova. Bert: Pre-training of deep bidirectional transformers for language understanding. In *NAACL-HLT*, 2019.

[40] Christos Louizos, Uri Shalit, Joris M Mooij, David Sontag, Richard S Zemel, and Max Welling. Causal effect inference with deep latent-variable models. In *NeurIPS*, 2017.

[41] Shakir Mohamed and Balaji Lakshminarayanan. Learning in implicit generative models. *arXiv*, 2016.

[42] David Newman. Bag of words data set. *UCI Machine Learning Respository*, 2008.

[43] Lizhen Nie, Mao Ye, Qiang Liu, and Dan Nicolae. Vcnet and functional targeted regularization for learning causal effects of continuous treatments. 2021.

[44] Sonali Parbhoo, Stefan Bauer, and Patrick Schwab. Ncore: Neural counterfactual representation learning for combinations of treatments. *arXiv*, 2021.

[45] Raghunathan Ramakrishnan, Pavlo O Dral, Matthias Rupp, and O Anatole Von Lilienfeld. Quantum chemistry structures and properties of 134 kilo molecules. *Scientific data*, 2014.

[46] Paul R Rosenbaum and Donald B Rubin. Reducing bias in observational studies using subclassification on the propensity score. *JASA*, 1984.

[47] Donald B Rubin. Causal inference using potential outcomes: Design, modeling, decisions. *Journal of the American Statistical Association*, 2005.

[48] Donald B Rubin. The design versus the analysis of observational studies for causal effects: parallels with the design of randomized trials. *Statistics in medicine*, 2007.

[49] Donald B Rubin and Neal Thomas. Matching using estimated propensity scores: relating theory to practice. *Biometrics*, 1996.

[50] Bernhard Schölkopf, Francesco Locatello, Stefan Bauer, Nan Rosemary Ke, Nal Kalchbrenner, Anirudh Goyal, and Yoshua Bengio. Toward causal representation learning. *Proceedings of the IEEE*, 2021.

[51] Patrick Schwab, Lorenz Linhardt, Stefan Bauer, Joachim M Buhmann, and Walter Karlen. Learning counterfactual representations for estimating individual dose-response curves. In *AAAI*, 2020.

[52] Patrick Schwab, Lorenz Linhardt, and Walter Karlen. Perfect match: A simple method for learning representations for counterfactual inference with neural networks. *arXiv*, 2018.

[53] Uri Shalit, Fredrik D Johansson, and David Sontag. Estimating individual treatment effect: generalization bounds and algorithms. In *ICML*, 2017.

[54] Claudia Shi, David Blei, and Victor Veitch. Adapting neural networks for the estimation of treatment effects. 2019.

[55] Brian K Shoichet. Interpreting steep dose-response curves in early inhibitor discovery. *Journal of medicinal chemistry*, 2006.

[56] Rahul Singh, Maneesh Sahani, and Arthur Gretton. Kernel instrumental variable regression. 2019.

[57] Yao-Hung Hubert Tsai, Shaojie Bai, Paul Pu Liang, J. Zico Kolter, Louis-Philippe Morency, and Ruslan Salakhutdinov. Multimodal transformer for unaligned multimodal language sequences. In *ACL*, 2019.

[58] Mark J Van Der Laan and Daniel Rubin. Targeted maximum likelihood learning. *The international journal of biostatistics*, 2006.

[59] Tyler J VanderWeele. Principles of confounder selection. *European journal of epidemiology*, 2019.

[60] Ashish Vaswani, Noam Shazeer, Niki Parmar, Jakob Uszkoreit, Llion Jones, Aidan N Gomez, Łukasz Kaiser, and Illia Polosukhin. Attention is all you need. In *NeurIPS*, 2017.

[61] Victor Veitch, Alexander D'Amour, Steve Yadlowsky, and Jacob Eisenstein. Counterfactual invariance to spurious correlations in text classification. 2021.

[62] Hao Wang, Hao He, and Dina Katabi. Continuously indexed domain adaptation. In *ICML*, 2020.

[63] Haohan Wang, Zeyi Huang, Hanlin Zhang, Yong Jae Lee, and Eric Xing. Toward learning human-aligned cross-domain robust models by countering misaligned features. 2022.

[64] Duncan J Watts and Steven H Strogatz. Collective dynamics of 'small-world'networks. *nature*, 1998.

[65] Yifan Wu, Ezra Winston, Divyansh Kaushik, and Zachary Lipton. Domain adaptation with asymmetrically-relaxed distribution alignment. In *ICML*, 2019.

[66] Guoqiang Xu, Cunxiang Yin, Yuchen Zhang, Yuncong Li, Yancheng He, Jing Cai, and Zhongyu Wei. Learning discriminative representation base on attention for uplift. In *Pacific-Asia Conference on Knowledge Discovery and Data Mining*, pages 200–211. Springer, 2022.

[67] Chengxuan Ying, Tianle Cai, Shengjie Luo, Shuxin Zheng, Guolin Ke, Di He, Yanming Shen, and Tie-Yan Liu. Do transformers really perform bad for graph representation? 2021.

[68] Jinsung Yoon, James Jordon, and Mihaela Van Der Schaar. Ganite: Estimation of individualized treatment effects using generative adversarial nets. In *ICLR*, 2018.

[69] Shuxi Zeng, Serge Assaad, Chenyang Tao, Shounak Datta, Lawrence Carin, and Fan Li. Double robust representation learning for counterfactual prediction, 2020.

[70] Hanlin Zhang, Yi-Fan Zhang, Weiyang Liu, Adrian Weller, Bernhard Schölkopf, and Eric P Xing. Towards principled disentanglement for domain generalization. *CVPR*, 2022.

[71] Yao Zhang, Alexis Bellot, and Mihaela Schaar. Learning overlapping representations for the estimation of individualized treatment effects. In *AISTATS*, 2020.

[72] Han Zhao, Shanghang Zhang, Guanhang Wu, José MF Moura, Joao P Costeira, and Geoffrey J Gordon. Adversarial multiple source domain adaptation. 2018.

Checklist

1. For all authors...
   (a) Do the main claims made in the abstract and introduction accurately reflect the paper's contributions and scope? [Yes] See the scope summarized in the abstract and introduction. The contributions are summarized point by point in Section 1.
   (b) Did you describe the limitations of your work? [Yes] See Section 6.
   (c) Did you discuss any potential negative societal impacts of your work? [Yes] See Section 6.
   (d) Have you read the ethics review guidelines and ensured that your paper conforms to them? [Yes] We have read the ethics review guidelines and ensured that our paper conforms to them.
2. If you are including theoretical results...
   (a) Did you state the full set of assumptions of all theoretical results? [Yes] See Section 3.
   (b) Did you include complete proofs of all theoretical results? [Yes] See Appendix C
3. If you ran experiments...
   (a) Did you include the code, data, and instructions needed to reproduce the main experimental results (either in the supplemental material or as a URL)? [Yes] We have included them in the Appendix E.

(b) Did you specify all the training details (e.g., data splits, hyperparameters, how they were chosen)? [Yes] We have included them in the Appendix E.

(c) Did you report error bars (e.g., with respect to the random seed after running experiments multiple times)? [Yes] We have reported our error bars in terms of standard deviation in the quantitative experiments.

(d) Did you include the total amount of compute and the type of resources used (e.g., type of GPUs, internal cluster, or cloud provider)? [Yes] We have included them in the Appendix E.

4. If you are using existing assets (e.g., code, data, models) or curating/releasing new assets...

(a) If your work uses existing assets, did you cite the creators? [Yes] We have cited the datasets (as well as the domain splits) we used in the **Datasets** and **Baselines** paragraphs in Section 5.

(b) Did you mention the license of the assets? [Yes] We have mentioned the lincense in Appendix E.

(c) Did you include any new assets either in the supplemental material or as a URL? [Yes] We have included the code, data, and instructions needed to reproduce the main experimental results in the supplemental material.

(d) Did you discuss whether and how consent was obtained from people whose data you're using/curating? [Yes] We have mentioned that we used the open-sourced datasets (as well as the domain splits) and cited them we used in the **Datasets** paragraph in Section 5.

(e) Did you discuss whether the data you are using/curating contains personally identifiable information or offensive content? [N/A]

5. If you used crowdsourcing or conducted research with human subjects...

(a) Did you include the full text of instructions given to participants and screenshots, if applicable? [No] We didn't use any crowdsourcing or conduct research with human subjects.

(b) Did you describe any potential participant risks, with links to Institutional Review Board (IRB) approvals, if applicable? [No] We didn't include any human participant.

(c) Did you include the estimated hourly wage paid to participants and the total amount spent on participant compensation? [No] We didn't include any human participant.

Exploring Transformer Backbones for Heterogeneous Treatment Effect Estimation – Appendix –

Table of Contents

A Extended Related Work

Neural Treatment Effect Estimation. There are many recent works on adapting neural networks to learn counterfactual representations for treatment effect estimation [34, 53, 40, 68, 8, 51, 43, 12]. To mitigate the imbalance of covariate representations across treatment groups, various approaches are proposed including optimizing distributional divergence (e.g. IPM including MMD, Wasserstein distance), entropy balancing [69] (converges to JSD between groups), counterfactual variance [71]. However, their domain-specific designs make them limited to different treatments as shown in Table 1: methods like VCNet [43] use a hand-crafted way to map a real-value treatment to an n-dimension vector with a constant mapping function, which is hard to converge under shifts of treatments (Table 4 in Appendix); models like TARNet [53] need an accurate estimation of the value interval of treatments. Moreover, previous estimators embed covariates to only one representation space by fully connected layers, tending to lose their connection and interactions [53, 35]. And it is non-trivial to adapt to the wider settings given existing ad hoc designs on network architectures. For example, the case with n treatments and m associated dosage requires $n \times m$ branches for methods like DRNet [51], which put a rigid requirement on the extrapolation capacity and infeasible given observational data.

Transformers and Attention Mechanisms Transformers [60] have demonstrated exemplary performance on a broad range of language tasks and their variants have been successfully adapted to representation learning over images [16], programming languages [10], and graphs [67] partly due to their flexibility and expressiveness. Their wide utility has motivated a line of work for general-purpose neural architectures [33, 32] that can be trained to perform tasks across various modalities like images, point clouds, audios and videos. But causal inference is fundamentally different from the above models' focus, i.e. supervised learning. And one of our goals is to explore the generalizability of attention-based models for TEE across domains with high-dimensional inputs, an important desideratum in causal representation learning [50].

Transformer for TEE. Currently, there are some attempts to use the embedding technique and attention mechanism for TEE Tasks [24, 66]. CETransformer [24] uses the embedding technique, but they only trivially learn covariate embeddings but not treatment embedding, while the latter is shown more important for TEE tasks. ANU [66] utilizes attention mechanisms to map the original covariate space X into a latent space Z in a single model, which is more similar to ours. We detail the difference between TransTEE and ANU [66] on both model designs and performance as follows: (i) The model structure is different. ANU performs cross-attention between z_x, and z_t, and no self-attention is applied. However, TransTEE performs self-attention on z_x, z_t respectively and then cross-attention is performed between z_x, z_t. When facing high-dimensional data, such as texts, images, and graphs, without multiple self-attention layers on z_x, z_t separately, the representations will be weak. That is why in machine translation, object detection, and segmentation tasks, the representations of images/texts will be firstly processed by multiple self-attention layers and then perform cross-attention with queries. We will verify this point in the following experiments. (ii) ANU cannot be applied to multi-treatment settings, which have been extensively studied recently [36, 8, 44]. The comparison experiments are in Section F.5.

Propensity Score. Most related works fundamentally rely on strongly ignorable conditions. Still even under ignorability, treatments may be selectively assigned according to propensities that depend on the covariates. To overcome the impact of such confounding, many statistical methods [5] like covariate adjustment [5], matching [49, 1], stratification [20], reweighting [27], g-computation [30], have been proposed. More recent approaches include propensity dropout [4], and multi-task Gaussian process [3]. Explicitly modeling the propensity score, which reflects the underlying policy for assigning treatments to subjects, has also shown to be effective in reasoning about the unobserved counterfactual outcomes and accounting for confounding. Based upon it, double robust estimators and targeted regularization are proposed to guarantee the consistency of estimated treatment effects under misspecification of either the outcome or propensity score model [38, 21]. There are also works using adversarial training for balanced representations [7, 37, 18]. However, most traditional approaches are restricted to binary treatments and the capacity of NNs for such problems have not been fully leveraged.

Domain Adaptation There are some close connections between causal inference and domain adaptation, in particular, out-of-distribution robustness. Intuitively, traditional domain adversarial training learns representations that are indistinguishable by the domain classifier by minimizing the worst-domain empirical error [22, 72, 63, 70]. The algorithmic insights can be handily translated to the TEE domain [53, 35, 19]. Here we also have the desideratum that covariate representations should

be balanced such that the selection bias is minimized and the effect is maximally determined by the treatment. Algorithmically, when the treatment is continuous, we connect our method to continuously indexed domain adaptation [62]. Our formulation and algorithm also serve to build connections to a diverse set of statistical thinking on causal inference and domain adaptation, of which much can be gained by mutual exchange of ideas [35]. Explicitly modeling the propensity score also seeks to connect causal inference with transfer learning to inspire domain adaptation methodology and holds the potential to handle a wider range of problems like hidden stratification in domain generalization, which we leave for future work.

B An Illustrative Example

To better understand the workflow with the above designs, we present a simple illustration here. Consider a use case in medicine effect estimation, where $\mathbf{x}$ contains p patient information, e.g., *Age, Sex, Blood Pressure (BP), and Previous infection condition (Prev)* with a corresponding causal graph (Figure 1). n medicines (treatments) are applied simultaneously and each medicine has a corresponding dosage. As shown in Figure 3, each covariate, treatment, and dosage will first be embedded to d-dimension representation by a specific **learnable embedding layer**. Each treatment embedding will be concatenated with its dosage embedding and the concatenated feature will be projected by a linear layer to produce d dimensional vectors. **Self-attention modules** optimizes these embeddings by aggregating contextual information. Specifically, attribute *Prev* is more related to *age* than *sex*, hence the attention weight of *Prev* feature to *age* feature is larger and the update of *Prev* feature will be more dependent on the *age* feature. Similarly, the interaction of multi-medicines is also attained by the self-attention module. The last **Cross-attention module** enables treatment-covariate interactions, which is shown in Figure 2 that, each medicine will assign a higher weight to relevant covariates especially confounders (*BP*) than irrelevant ones. Finally, we pool the resulted embedding and use one linear layer to predict the outcome.

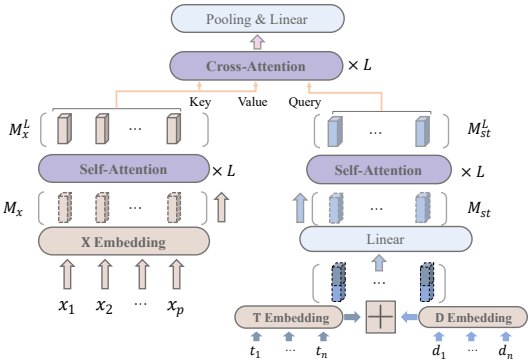

Figure 3: An Illustrative Example about the workflow of TransTEE.

C Details and Discussions about Propensity Score Modelling

We first discuss the fundamental differences and common goals between our algorithm and traditional ones: as a general approach to causal inference, TransTEE can be directly harnessed with traditional methods that estimate propensity scores by including hand-crafted features of covariates [30] to reduce biases through covariate adjustment [5], matching [49, 1], stratification [20], reweighting [27], g-computation [30], sub-classification [46], covariate adjustment [5], targeted regularization [58] or conditional density estimation [43] that create quasi-randomized experiments [13]. It is because the general framework provides an advantage to using an off-the-shelf propensity score regularizer for balancing covariate representations. Similar to the goal of traditional methods like inverse probability weighting and propensity score matching [5], which seeks to weigh a single observation to mimic the randomization effects with respect to the covariate from different treatment groups of interest.

Unlike previous works that use hand-crafted features or directly model the conditional density via maximum likelihood training, which is prone to high variance when handling high-dimensional, structured treatments [56] and can be problematic when we want to estimate a plausible propensity score from the generative model [41] (see the degraded performance of MLE in Table 2), TransTEE learns a propensity score network $\pi_\phi(t|\mathbf{x})$ via minimax bilevel optimization. The motivations for adversarial training between $\mu_\theta(\mathbf{x}, t)$ and $\pi_\phi(t|\mathbf{x})$ are three-fold: (i) it enforces the independence between treatment and covariate representations as shown in Proposition 1, which serves as algorithmic randomization in replace of costly randomized controlled trials [48] for overcoming selection bias

Table 3: **Performance of individualized treatment-dose response estimation** on the TCGA (D) dataset with different numbers of treatments. We report AMSE and standard deviation over 30 repeats. The selection bias on treatment and dosage are both set to be 2.0.

METHODS	#TREATMENT=1		#TREATMENT=2		#TREATMENT=3	
	IN-SAMPLE	OUT-SAMPLE	IN-SAMPLE	OUT-SAMPLE	IN-SAMPLE	OUT-SAMPLE
SCIGAN	5.6966 ± 0.0000	5.6546 ± 0.0000	2.0924 ± 0.0000	2.3067 ± 0.0000	4.3183 ± 0.0000	4.6231 ± 0.0000
TARNET(D)	0.7888 ± 0.0609	0.7908 ± 0.0606	1.4207 ± 0.0784	1.4206 ± 0.0777	3.1982 ± 0.5847	3.1920 ± 0.5746
DRNET(D)	0.8034 ± 0.0469	0.8052 ± 0.0466	1.3739 ± 0.0858	1.3738 ± 0.0853	2.8632 ± 0.4227	2.8558 ± 0.4143
VCNET(D)	0.1566 ± 0.0303	0.1579 ± 0.0301	0.2919 ± 0.0743	0.2918 ± 0.0737	0.6459 ± 0.1387	0.6493 ± 0.1397
TRANSTEE	0.0573 ± 0.0361	0.0585 ± 0.0358	**0.0550 ± 0.0137**	**0.0556 ± 0.0129**	0.2803 ± 0.0658	0.2768 ± 0.0639
TRANSTEE + TR	0.0495 ± 0.0176	0.0509 ± 0.0180	0.0663 ± 0.0268	0.0671 ± 0.0268	**0.2618 ± 0.0737**	**0.2577 ± 0.0726**
TRANSTEE + PTR	**0.0343 ± 0.0096**	**0.0355 ± 0.0094**	0.0679 ± 0.0252	0.0686 ± 0.0252	0.2645 ± 0.0702	0.2597 ± 0.0675

[13, 30]; (ii) it explicitly models propensity $\pi_\phi(t|\mathbf{x})$ to refine treatment representations and promote covariate adjustment [36]; and (iii) taking an adversarial domain adaptation perspective, the methodology is effective for learning invariant representations and further regularizes $\mu_\theta(\mathbf{x}, t)$ to be invariant to nuisance factors and may perform better empirically on some classes of distribution shifts [22, 53, 72, 35, 62].

Based on the above discussion, when treatments are discrete, one might consider directly applying heuristic methods like adversarial domain adaptation (see [22, 72] for algorithmic development guidelines). We note the heuristic nature of domain-adversarial methods (see [65] for clear failure cases), and a debunking of the common claim that [6] guarantees the robustness of such methods. Here, we focus on continuous TEE, a more general and challenging scenario, where we want to estimate ADRF, and propose two variants of $\mathcal{L}_\phi$ as an adversary for the outcome regression objective $\mathcal{L}_\theta$ in Eq. 1 accordingly. The process is shown in Eq. 2 below:

$$\min_\theta \max_\phi \mathcal{L}_\theta(\mathbf{x}, y, t) - \mathcal{L}_\phi(\mathbf{x}, t). \tag{2}$$

We refer to the above minimax game for algorithmic randomization in replace of costly randomized controlled trials. Such an algorithmic randomization based on neural representations using propensity score creates subgroups of different treated units as if they had been randomly assigned to different treatments such that conditional independence $T \perp\!\!\!\perp X \mid \pi(T|X)$ is enforced across strata and continuation, which approximates a random block experiment to the observed covariates [30].

Below we introduce two variants of $\mathcal{L}_\phi(\mathbf{x}, t)$:

Treatment Regularization (TR) is a standard MSE over the treatment space given the predicted treatment $\hat{t}_i$ and the ground truth t_i

$$\mathcal{L}_\phi^{TR}(\mathbf{x}, t) = \sum_{i=1}^{n} \left(t_i - \pi_\phi(\hat{t}_i|\mathbf{x}_i)\right)^2. \tag{3}$$

TR is explicitly matching the mean of the propensity score to that of the treatment. In an ideal case, the $\pi(t|\mathbf{x})$ should be uniformly distributed given different $\mathbf{x}$. However, the above treatment regularization procedure only provides matching for the mean of the propensity score, which can be prone to bad equilibriums and treatment misalignment [62]. Thus, we introduce the distribution of t and model the uncertainty rather than predicting a scalar t:

Probabilistic Treatment Regularization (PTR) is a probabilistic version of TR which models the mean μ (with a slight abuse of notation) and variance σ^2 of estimated treatment $\hat{t}_i$

$$\mathcal{L}_\phi^{PTR} = \sum_{i=1}^{n} \left[\frac{\left(t_i - \pi_\phi(\mu|\mathbf{x}_i)\right)^2}{2\pi_\phi(\sigma^2|\mathbf{x}_i)} + \frac{1}{2} \log \pi_\phi(\sigma^2|\mathbf{x}_i) \right]. \tag{4}$$

The PTR matches the whole distribution, i.e. both the mean and variance, of the propensity score to that of the treatment, which can be preferable in certain cases.

Equilibrium of the Minimax Game. We analyze that TR and PTR can align the first and second moment of continuous treatments at equilibrium respectively, and thus promote the independence between treatment t and covariate $\mathbf{x}$. To be clear, we denote $\mu_\theta(\mathbf{x}, t) := w_y \circ (\Phi_x(\mathbf{x}), \Phi_t(t))$ and $\pi_\phi(t|\mathbf{x}) := w_t \circ \Phi_x(\mathbf{x})$, which decompose the predictions into featurizers $\Phi_t : \mathcal{T} \to \mathcal{Z}_T, \Phi_x : \mathcal{X} \to$

$\mathcal{Z}_X$ and predictors $w_y : \mathcal{Z}_X \times \mathcal{Z}_T \to \mathcal{Y}, w_t : \mathcal{Z}_X \to \mathcal{T}$. For example, $\Phi_x(\mathbf{x})$ and $\Phi_t(t)$ can be the linear embedding layer and attention modules in our implementation. The propensity is computed on $\Phi_x(\mathbf{x})$, an intermediate feature representation of $\mathbf{x}$. Similarly, $\mu_\theta(\mathbf{x}, t)$ is computed from $\Phi_t(t)$ and $\Phi_x(\mathbf{x})$. For the ease of our analysis below, we assume the predictors w_t, w_x are fixed.

Proposition 1. *(The optimum of propensity score model) In the equilibrium of the game, assuming the outcome prediction model is fixed, then the optimum of TR is achieved when* $\mathbb{E}[\Phi_t(t)|\Phi_x(\boldsymbol{x})] = \mathbb{E}[\Phi_t(t)], \forall\ \Phi_x(\boldsymbol{x})$ *via matching the mean of propensity score* $\pi(\Phi_t(t)|\Phi_x(\boldsymbol{x}))$ *and the marginal distribution* $p(\Phi_x(\boldsymbol{x}))$ *and the optimum discriminator of PTR is achieved via matching both the mean and variance such that* $\mathbb{E}[\Phi_t(t)|\Phi_x(\boldsymbol{x})] = \mathbb{E}[\Phi_t(t)], \mathbb{V}[\Phi_t(t)|\Phi_x(\boldsymbol{x})] = \mathbb{V}[\Phi_t(t)],\ \forall\ \Phi_x(\boldsymbol{x})$.

Proof. The proof concerns the analysis of the Equilibrium of the Minimax Game. It is a special case of [62] when there are only two players, i.e. μ_θ and π_ϕ. We represent treatments explicitly and interpret the connections with combating selection biases. Given the outcome regression model μ_θ fixed, the optimal propensity score model π^* is

$$\begin{aligned}
\pi^* &= \arg\min_{\pi} \mathcal{L}_\phi(\Phi_x(\mathbf{x}), \Phi_t(t)) \\
&= \arg\min_{\pi} \mathbb{E}_{(\Phi_x(\mathbf{x}),\Phi_t(t))\sim p(\Phi_x(\mathbf{x}),\Phi_t(t))} \left(\Phi_t(t) - \pi_\theta\left(\Phi_t(\hat{t})|\mathbf{x}\right)\right)^2 \\
&= \arg\min_{\pi} \mathbb{E}_{\Phi_x(\mathbf{x})\sim p(\Phi_x(\mathbf{x}))} \mathbb{E}_{\Phi_t(t)\sim p(\Phi_t(t)|\Phi_x(\mathbf{x}))} \left(\Phi_t(t) - \pi_\theta\left(\Phi_t(\hat{t})|\mathbf{x}\right)\right)^2.
\end{aligned} \tag{5}$$

The inner minimum is achieved at $\pi^*_\theta\left(\Phi_t(\hat{t})|\mathbf{x}\right) = \mathbb{E}_{\Phi_t(t)\sim p(\Phi_t(t)|\Phi_x(\mathbf{x}))}[\Phi_t(t)]$ given the following quadratic form:

$$\begin{aligned}
&\mathbb{E}_{(\Phi_x(\mathbf{x}),\Phi_t(t))\sim p(\Phi_x(\mathbf{x}),\Phi_t(t))} \left(\Phi_t(t) - \pi_\theta\left(\Phi_t(\hat{t})|\Phi_{\mathbf{x}}(\mathbf{x})\right)\right)^2 = \\
&\mathbb{E}_{\Phi_t(t)\sim p(\Phi_t(t)|\Phi_x(\mathbf{x}))}[\Phi_t(t)^2] - 2\pi_\theta\left(\Phi_t(\hat{t})|\mathbf{x}\right) \mathbb{E}_{\Phi_t(t)\sim p(\Phi_t(t)|\Phi_x(\mathbf{x}))}[\Phi_t(t)] + \pi_\theta\left(\Phi_t(\hat{t})|\mathbf{x}\right)^2.
\end{aligned} \tag{6}$$

We assume the above optimum condition of the propensity score model always holds with respect to the outcome regression model during training, then the minimax game in Eq. 2 can be converted to maximizing the inner loop:

$$\begin{aligned}
&\max_{\phi} -\mathcal{L}_\phi(\mathbf{x}, \Phi_t(t)) = \mathcal{L}_{\phi^*}(\Phi_x(\mathbf{x}), \Phi_t(t)) \\
&= \mathbb{E}_{(\Phi_x(\mathbf{x}),\Phi_t(t))\sim p(\Phi_x(\mathbf{x}),\Phi_t(t))} \left(\Phi_t(t) - \mathbb{E}_{\Phi_t(t)\sim p(\Phi_t(t)|\Phi_x(\mathbf{x}))}[\Phi_t(t)]\right)^2 \\
&= \mathbb{E}_{\Phi_x(\mathbf{x})\sim p(\Phi_x(\mathbf{x}))} \mathbb{E}_{\Phi_t(t)\sim p(\Phi_t(t)|\Phi_x(\mathbf{x}))\sim p(\Phi_x(\mathbf{x}),\Phi_t(t))} \left(\Phi_t(t) - \mathbb{E}_{\Phi_t(t)\sim p(\Phi_t(t)|\Phi_x(\mathbf{x}))}[\Phi_t(t)]\right)^2 \\
&= \mathbb{E}_{\Phi_x(\mathbf{x})\sim p(\Phi_x(\mathbf{x}))} \mathbb{V}_{\Phi_t(t)\sim p(\Phi_t(t)|\Phi_x(\mathbf{x}))}[\Phi_t(t)] = \mathbb{E}_{\Phi_x(\mathbf{x})} \mathbb{V}[\Phi_t(t)|\Phi_x(\mathbf{x})].
\end{aligned} \tag{7}$$

Next we show the difference between Eq. 7 and the variance of the treatment $\mathbb{V}[\Phi_t(t)]$:

$$\begin{aligned}
&\mathbb{E}_{\Phi_x(\mathbf{x})\sim p(\Phi_x(\mathbf{x}))} \mathbb{V}_{\Phi_t(t)\sim p(\Phi_t(t)|\Phi_x(\mathbf{x}))}[\Phi_t(t)] - \mathbb{V}[\Phi_t(t)] \\
=&\mathbb{E}_{\Phi_x(\mathbf{x})\sim p(\Phi_x(\mathbf{x}))}[\mathbb{E}[\Phi_t(t)^2|\Phi_x(\mathbf{x})] - \mathbb{E}[\Phi_t(t)|\Phi_x(\mathbf{x})]^2] - (\mathbb{E}[\Phi_t(t)^2] - \mathbb{E}[\Phi_t(t)]^2) \\
=&\mathbb{E}[\Phi_t(t)]^2 - \mathbb{E}_{\Phi_x(\mathbf{x})}[\mathbb{E}[\Phi_t(t)|\Phi_x(\mathbf{x})]^2] = \mathbb{E}_{\Phi_x(\mathbf{x})}[\mathbb{E}[\Phi_t(t)|\Phi_x(\mathbf{x})]]^2 - \mathbb{E}_{\Phi_x(\mathbf{x})}[\mathbb{E}[\Phi_t(t)|\Phi_x(\mathbf{x})]^2] \\
\leq&\mathbb{E}_{\Phi_x(\mathbf{x})}[\mathbb{E}[\Phi_t(t)|\Phi_x(\mathbf{x})]^2] - \mathbb{E}_{\Phi_x(\mathbf{x})}[\mathbb{E}[\Phi_t(t)|\Phi_x(\mathbf{x})]^2] = 0
\end{aligned} \tag{8}$$

where the last inequality is by Jensen's inequality and the convexity of $\Phi_t(t)^2$. The optimum is achieved when $\mathbb{E}[\Phi_t(t)|\Phi_x(\mathbf{x})]$ is constant w.r.t $\Phi_x(\mathbf{x})$ and so $\mathbb{E}[\Phi_t(t)|\Phi_x(\mathbf{x})] = \mathbb{E}[\Phi_t(t)],\ \forall \Phi_x(\mathbf{x})$.

The proof process for PTR is similar but includes the derivation of variance matching.

$$\begin{aligned}
\pi^* &= \arg\min_{\pi} \mathcal{L}_\phi(\Phi_x(\mathbf{x}), \Phi_t(t)) \\
&= \arg\min_{\pi} \mathbb{E}_{(\Phi_x(\mathbf{x}),\Phi_t(t))\sim p(\Phi_x(\mathbf{x}),\Phi_t(t))} \left(\frac{(\mathbb{E}[\Phi_t(t)|\Phi_x(\mathbf{x})] - \Phi_t(t))^2}{2\mathbb{V}[\Phi_t(t)|\Phi_x(\mathbf{x})]} + \frac{\log \mathbb{V}[\Phi_t(t)|\Phi_x(\mathbf{x})]}{2}\right) \\
&= \arg\min_{\pi} \mathbb{E}_{\Phi_x(\mathbf{x})} \mathbb{E}_{\Phi_t(t)} \left(\frac{(\mathbb{E}[\Phi_t(t)|\Phi_x(\mathbf{x})] - \Phi_t(t))^2}{2\mathbb{V}[\Phi_t(t)|\Phi_x(\mathbf{x})]} + \frac{\log \mathbb{V}[\Phi_t(t)|\Phi_x(\mathbf{x})]}{2}\right),
\end{aligned} \tag{9}$$

where $\mathbb{E}_{\Phi_x(\mathbf{x})}$ and $\mathbb{E}_{\Phi_t(t)}$ denote $\mathbb{E}_{\Phi_x(\mathbf{x})\sim p(\Phi_x(\mathbf{x}))}$ and $\mathbb{E}_{\Phi_t(t)\sim p(\Phi_t(t)|\Phi_x(\mathbf{x}))}$ respectively for brevity. The first term can be reduce to a constant given the definition of variance:

$$\begin{aligned}&\mathbb{E}_{\Phi_x(\mathbf{x})\sim p(\Phi_x(\mathbf{x}))}\mathbb{E}_{\Phi_t(t)\sim p(\Phi_t(t)|\Phi_x(\mathbf{x}))}\left(\frac{(\mathbb{E}[\Phi_t(t)|\mathbf{x}]-\Phi_t(t))^2}{2\mathbb{V}[\Phi_t(t)|\mathbf{x}]}\right)\\&=\mathbb{E}_{\Phi_x(\mathbf{x})\sim p(\Phi_x(\mathbf{x}))}\left(\frac{\mathbb{V}[\Phi_t(t)|\mathbf{x}]}{2\mathbb{V}[\Phi_t(t)|\mathbf{x}]}\right)=\frac{1}{2}.\end{aligned} \tag{10}$$

The second term can be upper bounded by using Jensen's inequality:

$$\begin{aligned}&\mathbb{E}_{\Phi_x(\mathbf{x})\sim p(\Phi_x(\mathbf{x}))}\mathbb{E}_{\Phi_t(t)\sim p(\Phi_t(t)|\Phi_x(\mathbf{x}))}\left(\frac{\log\mathbb{V}[\Phi_t(t)|\mathbf{x}]}{2}\right)\\&\leq\frac{1}{2}\log\left(\mathbb{E}_{\Phi_x(\mathbf{x})\sim p(\Phi_x(\mathbf{x}))}[\mathbb{V}[\Phi_t(t)|\Phi_x(\mathbf{x})]]\right)\\&\leq\frac{1}{2}\log\left(\mathbb{V}[\Phi_t(t)]\right).\end{aligned} \tag{11}$$

Combining Eq. 10 and Eq. 11, the optimum $\frac{1}{2}+\frac{1}{2}\log\left(\mathbb{V}[\Phi_t(t)]\right)$ is achieved when $\mathbb{E}[\Phi_t(t)|\Phi_x(\mathbf{x})]$, $\mathbb{V}[\Phi_t(t)|\Phi_x(\mathbf{x})]$ is constant w.r.t $\Phi_x(\mathbf{x})$ and so $\mathbb{E}[\Phi_t(t)|\Phi_x(\mathbf{x})]=\mathbb{E}[\Phi_t(t)], \mathbb{V}[\Phi_t(t)|\Phi_x(\mathbf{x})]=\mathbb{V}[\Phi_t(t)],\ \forall\Phi_x(\mathbf{x})$ according to the equality conditions of the first and second inequality in Eq. 11, respectively. □

D Analysis of the Failure Cases over Treatment Distribution Shifts

As shown in Figure 4 (a,c), with the shifts of the treatment interval, the estimation performance of DRNet and TARNet decline significantly. VCNet achieves ∞ estimation error when $h=5$ partly because its hand-craft projection matrix can only process values near $[0,1]$. Another problem brought by this assumption is the extrapolation dilemma, which can be seen in Figure 4(b). When training on $t\in[0,1.75]$, these discrete approximation methods cannot transfer to new distribution $t\in(1.75,2.0]$. These unseen treatments are rounded down to the nearest neighbors t' in T and be seemed the same as t'. We conduct ablation about the treatment embedding as in Table 4 in Appendix. Such a simple fix (VCNet+Embeddings) removes the demand on a fixed interval constraint to treatments and attains superior performance on both interpolation and extrapolation settings. The result clearly shows the pitfalls of hand-crafted feature mapping for TEE. We highlight that it is neglected by most existing works [51, 43, 54, 24]. Extrapolation is still a challenging open problem. We can see that no existing work does well when training and test treatment intervals have big gaps. However, the empirical evidence validates the improved effectiveness of TransTEE that uses learnable embeddings to map continuous treatments to hidden representations.

Below we show the assumption that the value of treatments or dosages are in a fixed interval $[l,h]$ is sub-optimal and thus these methods get poor extrapolation results. For simplicity, we only consider a data sample has only one continuous treatment t and the result is similar for continuous dosage.

Proposition 2. *Given a data sample* $(\mathbf{x},t,y)$*, where* $\mathbf{x}\in\mathbb{R}^d, t\in[l,h], y\in\mathbb{R}$*. Assume* μ *is*

a L-Lipschitz function over $(\mathbf{x}, t) \in \mathbb{R}^{d+1}$*, namely* $|\mu(\mathbf{u}) - \mu(\mathbf{v})| \leq L\|\mathbf{u} - \mathbf{v}\|$*. Partitioning* $[l, h]$ *uniformly into* δ *sub-interval, and then get* $T = \left[l + \frac{h-l}{\delta} * 0, l + \frac{h-l}{\delta} * 1, ..., l + \frac{h-l}{\delta} * \delta\right]$*. Previous studies most rounding down a treatment* t *to its nearest value in* T *(either* $l + \left\lfloor \frac{t\delta}{h-l} \right\rfloor \frac{h-l}{\delta}$ *or* $l + \left\lceil \frac{t\delta}{h-l} \right\rceil \frac{h-l}{\delta}$*) and use* $|T|$ *branches to approximate the entire continuum* $[l, h]$*. The approximation error can be bounded by*

$$
\begin{aligned}
&\max\left\{\mu\left(\mathbf{x}, \left\lfloor \frac{t\delta}{h-l} \right\rfloor \frac{h-l}{\delta}\right) - \mu(\mathbf{x}, t), \mu\left(\mathbf{x}, \left\lceil \frac{t\delta}{h-l} \right\rceil \frac{h-l}{\delta}\right) - \mu(\mathbf{x}, t)\right\} \\
&\leq \max\left\{L\left(\left|\left\lfloor \frac{t\delta}{h-l} \right\rfloor \frac{h-l}{\delta} - t\right|\right), L\left(\left|\left\lceil \frac{t\delta}{h-l} \right\rceil \frac{h-l}{\delta} - t\right|\right)\right\} \\
&\leq L\frac{h-l}{\delta}
\end{aligned}
\tag{12}
$$

The bound is affected by both the number of branches δ and treatment interval $[l, h]$. However, as far as we know, most previous works ignore the impacts of the treatment interval $[l, h]$ and adopt a simple but much stronger assumption that treatments are all in the interval $[0, 1]$ [43] or a fixed interval [51]. These observations well manifest the motivation of our general framework for TEE without the need for treatment-specific architectural designs.

Table 4: **Experimental results comparing NN-based methods on simulated datasets.** Numbers reported are AMSE of test data based on 100 repeats, and numbers after $\pm$ are the estimated standard deviation of the average value. For Extrapolation ($h = 2$), models are trained with $t \in [0, 1.75]$ and tested in $t \in [0, 2]$. For Extrapolation ($h = 5$), models are trained with $t \in [0, 4]$ and tested in $t \in [0, 5]$

METHODS	VANILLA	VANILLA ($h = 5$)	EXTRAPOLATION ($h = 2$)	EXTRAPOLATION ($h = 5$)
TARNET [53]	0.045 ± 0.0009	0.3864 ± 0.04335	0.0984 ± 0.02315	0.3647 ± 0.03626
DRNET [51]	0.042 ± 0.0009	0.3871 ± 0.03851	0.0885 ± 0.00094	0.3647 ± 0.03625
VCNET[43]	0.018 ± 0.0010	NAN	0.0669 ± 0.05227	NAN
VCNET+EMBEDDINGS	0.013 ± 0.00465	0.0167 ± 0.01150	0.0118 ± 0.00482	0.0178 ± 0.00887

E Additional Experimental Setups

E.1 Experimental Settings

Datasets. Since the true counterfactual outcome (or ADRF) are rarely available for real-world data, we use synthetic or semi-synthetic data for empirical evaluation. for continuous treatments, we use one synthetic dataset and two semi-synthetic datasets: the *IHDP* and *News* datasets. For treatment with continuous dosages, we obtain covariates from a real dataset TCGA [9] and generate treatments, where each treatment is accompanied by a dosage. The resulting dataset is named *TCGA (D)*. Following [36], datasets for structured treatments include *Small-World (SW)*, which contains $1,000$ uniformly sampled covariates and 200 randomly generated Watts–Strogatz small-world graphs [64] as treatments, and *TCGA (S)*, which uses $9,659$ gene expression measurements of cancer patients [9] for covariates and $10,000$ sampled molecules from the QM9 dataset [45] as treatments. For the study on language models, we use *The Enriched Equity Evaluation Corpus (EEEC)* dataset [19].

Baselines. Baselines for **continuous and binary** treatments include TARnet [53], Dragonnet [54], DRNet [51], FlexTENet [12], and VCNet [43]. SCIGAN [8] is chosen as the baseline for **continuous dosages**. Besides, we revise DRNet [51], TARNet [53], and VCNet [43] to DRNet (D), TARNet (D), VCNet (D), respectively, which enable multiple treatments and dosages. Specifically, DRNet (D) has T main flows, each corresponding to a treatment and is divided into B_D branches for continuous dosage. Baselines for **structured** treatments include Zero [36], GNN [36], GraphITE [25], and SIN [36]. To compare the performance of different frameworks fairly, all of the models regress on the outcome with empirical samples without any regularization. For MLE training of the propensity score model, the objective is the negative log-likelihood: $\mathcal{L}_\phi := -\frac{1}{n}\sum_{i=1}^{n} \log \pi_\phi(t_i|\mathbf{x}_i)$.

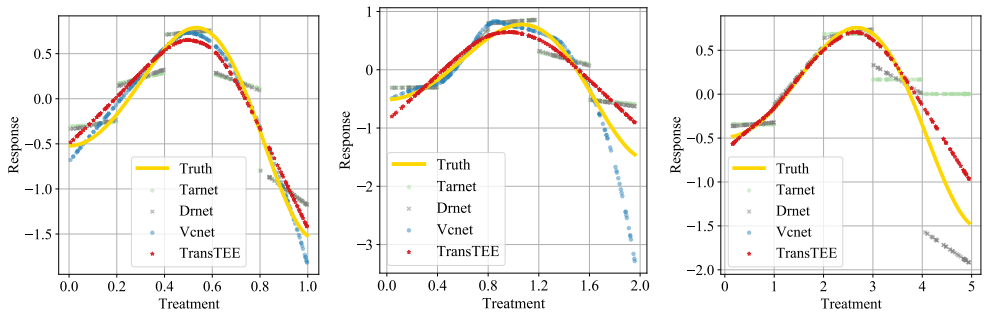

(a) $h = 1$ in training and testing. (b) $h = 1.75$ in traning and $h = 2$ in testing (extrapolation). (c) $h = 5$ in training and testing.

Figure 4: **Estimated ADRF on the synthetic dataset**, where treatments are sampled from an interval $[l, h]$, where $l = 0$.

Evaluation Metric. For **continuous and binary** treatments, we use the average mean squared error on the test set. For **structured** treatments, following [36], we rank all treatments by their propensity $\pi(t|\mathbf{x})$ in a descending order. Top K treatments are selected and the treatment effect of each treatment pair is evaluated by unweighted/weighted expected Precision in Estimation of Heterogeneous Effect (PEHE) [36], where the WPEHE@K accounts for the fact that treatment pairs that are less likely to have higher estimation errors should be given less importance. For **multiple treatments and dosages**, AMSE is calculated over all dosage and treatment pairs, resulting in $\text{AMSE}_{\mathcal{D}}$.

All the assets (i.e., datasets and the codes for baselines) we use include a MIT license containing a copyright notice and this permission notice shall be included in all copies or substantial portions of the software. We conduct all the experiments on a machine with i7-8700K CPU, 32G RAM, and four Nvidia GeForce RTX2080Ti (10GB) GPU cards.

E.2 Detail Evaluation Metrics.

$$\text{AMSE}_{\mathcal{T}} = \frac{1}{N}\sum_{i=1}^{N}\int_{\mathcal{T}}\left[\hat{f}(\mathbf{x}_i, t) - f(\mathbf{x}_i, t)\right]\pi(t)dt \tag{13}$$

$$\begin{aligned}\text{UPEHE@K} &= \frac{1}{N}\sum_{i=1}^{N}\left[\frac{1}{C_K^2}\sum_{t,t'}\left[\hat{f}(\mathbf{x}_i, t, t') - f(\mathbf{x}_n, t, t')\right]^2\right] \\ \text{WPEHE@K} &= \frac{1}{N}\sum_{i=1}^{N}\left[\frac{1}{C_K^2}\sum_{t,t'}\left[\hat{f}(\mathbf{x}_i, t, t') - f(\mathbf{x}_i, t, t')\right]^2 p(t|\mathbf{x})p(t'|\mathbf{x})\right],\end{aligned} \tag{14}$$

$$\text{AMSE}_{\mathcal{D}} = \frac{1}{NT}\sum_{i=1}^{N}\sum_{t=1}^{T}\int_{\mathcal{D}}\left[\hat{f}(\mathbf{x}_i, t, s) - f(\mathbf{x}_n, t, s)\right]\pi(s)dt \tag{15}$$

E.3 Network Structure and Parameter Setting

Table. 5 and Table. 6 show the detail of TransTEE architecture and hyper-parameters. For all the synthetic and semi-synthetic datasets, we tune parameters based on 20 additional runs. In each run, we simulate data, randomly split it into training and testing, and use AMSE on testing data for evaluation. For fair comparisons, in all experiments, the model size of TransTEE is less than or similar to baselines.

Table 5: **Architecture details of TransTEE**, where p is the number of covariates.

Module	Covariates	Treatment
Embedding Layer	[Linear]	[Linear]
Output Size	Bsz $\times$ p $\times$ #Emb	$bsz \times 1 \times$ # Emb
Self-Attention	[Multi-head Att, BatchNorm, Linear, BatchNorm] $\times$ #Layers	[Multi-head Att, BatchNorm, Linear, BatchNorm] $\times$ #Layers
Output Size	Bsz $\times$ p $\times$ #Emb	Bsz $\times$ 1 $\times$ #Emb
Cross-Attention	[Multi-head Att, BatchNorm, Linear, BatchNorm] $\times$ #Layers	
Output Size	Bsz $\times$ 1 $\times$ #Emb	
Projection Layer	[Linear]	
Output Size	Bsz $\times$ 1	

Table 6: **Hyper-parameters on different datasets**. Bsz indicates the batch size, # Emb indicates the embedding dimension, Lr. S indicates the scheduler of the learning rate (Cos is the cosine annealing Learning rate).

Dataset	Bsz	# Emb	# Layers	# Heads	Lr	Lr. S
Simu	500	10	1	2	0.01	Cos
IHDP	128	10	1	2	0.0005	Cos
News	256	10	1	2	0.01	Cos
SW	500	16	1	2	0.01	None
TCGA	1000	48	3	4	0.01	None

E.4 Simulation details.

Synthetic Dataset [43]. The synthetic dataset contains 500 training points and 200 testing points. Data is generated as follows: $x_j \sim \text{Unif}[0,1]$, where x_j is the j-th dimension of $x \in \mathbb{R}^6$, and

$$\tilde{t}|x = \frac{10\sin\left(\max(x_1,x_2,x_3)\right) + \max(x_3,x_4,x_5)^3}{1+(x_1+x_5)^2} + \sin(0.5x_3)\left(1+\exp(x_4-0.5x_3)\right) + x_3^2 + 2\sin(x_4) + 2x_5 - 6.5 + \mathcal{N}(0,0.25)$$

$$y|x,t = \cos(2\pi(t-0.5))\left(t^2 + \frac{4\max(x_1,x_6)^3}{1+2x_3^2}\right) + \mathcal{N}(0,0.25)$$

where $t = (1+\exp(-\tilde{t}))^{-1}$.

for treatment in $[0,h]$, we revised it to $t = (1+\exp -\tilde{t})^{-1} * h$,

IHDP [26] is a semi-synthetic dataset containing 25 covariates, 747 observations and binary treatments. For treatments in $[0,1]$, we follow VCNet [43] and generate treatments and responses by:

$$\tilde{t}|x = \frac{2x_1}{1+x_2} + \frac{2\max(x_3,x_5,x_6)}{0.2+\min(x_3,x_5,x_6)} + 2\tanh\left(5\frac{\sum_{i\in S_{dis,2}}(x_i-c_2)}{|S_{dis,2}|} - 4 + \mathcal{N}(0,0.25)\right)$$

$$y|x,t = \frac{\sin(3\pi t)}{1.2-t}\left(\tanh\left(5\frac{\sum_{i\in S_{dis,1}}(x_i-c_1)}{|S_{dis,1}|}\right) + \frac{\exp(0.2(x_1-x_6))}{0.5+5\min(x_2,x_3,x_5)}\right) + \mathcal{N}(0,0.25),$$

where $t = (1+\exp(-\tilde{t}))^{-1}$, $S_{con} = \{1,2,3,5,6\}$ is the index set of continuous features, $S_{dis,1} = \{4,7,8,9,10,11,12,13,14,15\}$, $S_{dis,2} = \{16,17,18,19,20,21,22,23,24,25\}$ and $S_{dis,1} \bigcup S_{dis,2} = [25] - S_{con}$. Here $c_1 = \mathbb{E}\left[\frac{\sum_{i\in S_{dis,1}} x_i}{|S_{dis,1}|}\right]$,$c_2 = \mathbb{E}\left[\frac{\sum_{i\in S_{dis,2}} x_i}{|S_{dis,2}|}\right]$. To allow

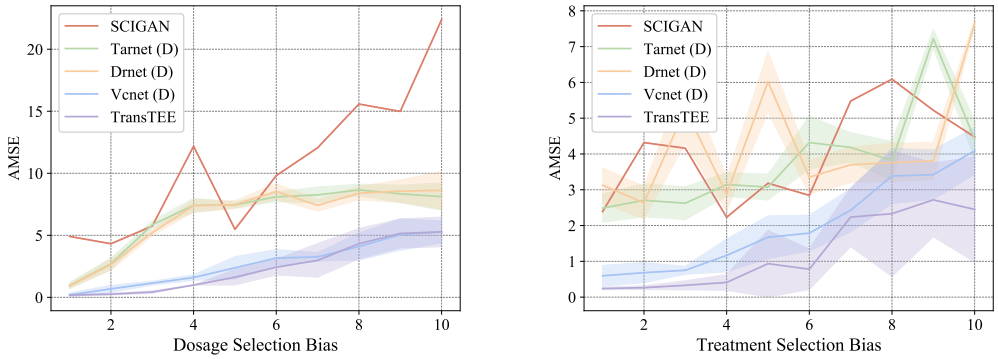

(a) Performance with different dosage selection bias. (b) Performance with different treatment selection bias.

Figure 5: Performance of five methods on TCGA (D) dataset with varying bias levels.

comparison on various treatment intervals $t \in [0, h]$, treatments and responses are generated by:

$$t = (1 + \exp(-\tilde{t}))^{-1} * h$$

$$y|x,t = \frac{\sin(3\pi t/h)}{1.2 - t/h}\left(\tanh\left(5\frac{\sum_{i\in S_{dis,1}}(x_i - c_1)}{|S_{dis,1}|}\right) + \frac{\exp(0.2(x_1 - x_6))}{0.5 + 5\min(x_2, x_3, x_5)}\right) + \mathcal{N}(0, 0.25),$$

where the orange part is the only different compared to the generalization of vanilla IHDP dataset ($h = 1$). Note that $S_{dis,1}$ only impacts outcome that serves to be noisy covariates; $S_{dis,2}$ contains pre-treatment covariates that only impact treatments, which also serves to be instrumental variables. This allows us to observe the improvement using TransTEE when noisy covariates exist. Following [26] covariates are standardized with mean 0 and standard deviation 1.

News. The News dataset consists of 3000 randomly sampled news items from the NY Times corpus [42] and was originally introduced as a benchmark in the binary treatment setting. We generate the treatment and outcome in a similar way as [43] but with a dynamic range or treatment intervals $[0, h]$. We first generate $v_1', v_2', v_3' \sim \mathcal{N}(0, 1)$ and then set $v_i = v_i'/\|v_i'\|_2; i \in \{1, 2, 3\}$. Given x, we generate t from Beta $\left(2, \left|\frac{v_3^\top x}{2v_2^\top x}\right|\right) * h$.And we generate the outcome by

$$y'|x,t = \exp\left(\frac{v_2^\top x}{v_3^\top x} - 0.3\right)$$

$$y|x,t = 2(\max(-2, \min(2, y')) + 20v_1^\top x) * \left(4(t - 0.5)^2 + \sin\left(\frac{\pi}{2}t\right)\right) + \mathcal{N}(0, 0.5)$$

TCGA (D) [8] We obtain covariates x from a real dataset *The Cancer Genomic Atlas (TCGA)* and consider 3 treatments, where each treatment is accompanied by one dosage and a set of parameters, v_1^t, v_2^t, v_3^t. For each run, we randomly sample a vector, $u_i^t \sim \mathcal{N}(0, 1)$ and then set $v_i^t = u_i^t/\|u_i^t\|$ where $\|\cdot\|$ is Euclidean norm. The shape of the response curve for each treatment, $f_t(x, s)$ is given in Table 7. We add $\epsilon \sim \mathcal{N}(0, 0.2)$ noise to the outcomes. Interventions are assigned by sampling a dosage, d_t, for each treatment from a beta distribution, $d_t|x \sim \text{Beta}(\alpha, \beta_t)$. $\alpha \geq 1$ controls the dosage selection bias ($\alpha = 1$ gives the uniform distribution). $\beta_t = \frac{\alpha-1}{s_t^*} + 2 - \alpha$, where s_t^* is the optimal dosage[2] for treatment t. We then assign a treatment according to $t_f|x \sim$ Categorical(Softmax($\kappa f(x, s_t)$)) where increasing κ increases selection bias, and $\kappa = 0$ leads to random assignments. The factual intervention is given by (t_f, s_{t_f}). Unless otherwise specified, we set $\kappa = 2$ and $\alpha = 2$.

For structural treatments, we first define the **Baseline effect** [8]. For each run of the experiment, we randomly sample a vector $u_0 \sim \text{Unif}[0, 1]$, and set $v_0 = u_0/\|u_o\|$, where $\|\cdot\|$ is the Euclidean norm. The baseline effect is defined as

$$\mu_0(x) = v_0^\top x$$

[2]For symmetry, if $s_t^* = 0$, we sample s_t^* from $1-\text{Beta}(\alpha, \beta_t)$ where β_t is set as though $s_t^* = 1$.

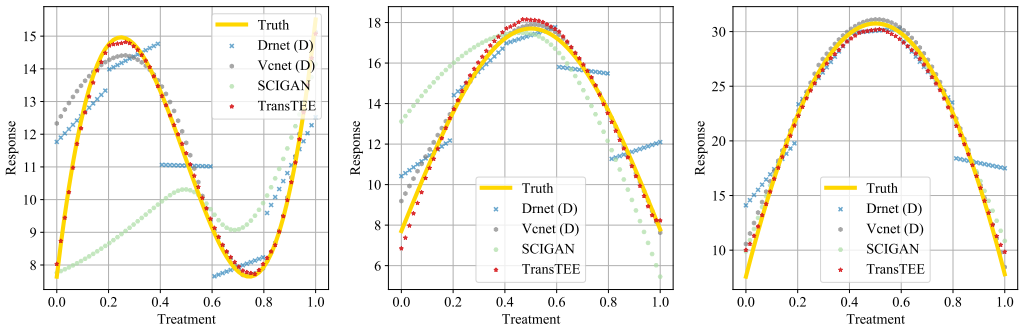

(a) Estimated ADRF for t_1. (b) Estimated ADRF for t_2. (c) Estimated ADRF for t_3.

Figure 6: **Estimated ADRF** on the test set from a typical run of DRNet (D), TARNet (D), VCNet (D), and SCIGAN. All of these methods are well optimized. TransTEE can well estimate the dosage-response curve for all treatments.

Table 7: **Dose response curves used to generate semi-synthetic outcomes for patient features** x. In the experiments, we set $C = 10$. v_1^t, v_2^t, v_3^t are the parameters associated with each treatment t.

Treatment	Dose-Response	Optimal dosage
1	$f_1(x,s) = C\left((v_1^1)^\top x + 12(v_3^1)^\top xs - 12(v_3^1)^\top xs^2\right)$	$s_1^* = \frac{(v_2^1)^\top x}{2(v_3^1)^\top x}$
2	$f_2(x,s) = C\left((v_1^2)^\top x + \sin\left(\pi(\frac{v_2^{2\top} x}{v_3^{2\top} x}s)\right)\right)$	$s_2^* = \frac{(v_3^2)^\top x}{2(v_2^2)^\top x}$
3	$f_3(x,s) = C\left((v_1^3)^\top x + 12s(s-b)^2, \text{where } b = 0.75\frac{(v_2^3)^\top x}{(v_3^3)^\top x}\right)$	$\frac{b}{3}$ if $b \geq 0.75$ else 1

Small-World [36]. 20-dimensional multivariate covariates are uniformly sampled according to $x_i \sim \text{Unif}[-1, 1]$. There are $1,000$ units in in-sample dataset, and 500 in the out-sample one. *Graph interventions* For each graph intervention, a number of nodes between 10 and 120 are uniformly sampled, the number of neighbors for each node is between 3 and 8, and the probability of rewiring each edge is between 0.1 and 1. Watts–Strogatz small-world graphs are repeatedly generated until a connected one is get. Each vertex has one feature, i.e. its degree centrality. A graph's node connectivity is denoted as $\nu(\mathcal{G})$ and its average shortest path length as $\ell(\mathcal{G})$. Similar for the baseline effect, two randomly sampled vectors v_ν, v_ℓ are generated. Then, given an assigned graph treatment $\mathcal{G}$ and a covariate vector x, the *outcome* is generated by

$$y = 100\mu_0(x) + 0.2\nu(\mathcal{G})^2 \cdot v_\nu^\top x + \ell(\mathcal{G}) \cdot \nu_\ell^\top x + \epsilon, \epsilon \sim \mathcal{N}(0, 1)$$

TCGA (S) [36] We use $9,659$ gene expression measurements of cancer patients for covariates. The in-sample and datasets consist of $5,000$ units and the out-sample one of $4,659$ units, respectively. Each unit is a covariate vector $x \in \mathbb{R}^{4000}$ and these units are split randomly into in- and out-sample datasets in each run randomly. For each covariate vector x, its 8-dimensional PCA components $x^{\text{PCA}} \in \mathbb{R}^8$ is computed. *Graph interventions* We randomly sample $10,000$ molecules from the Quantum Machine 9 (QM9) dataset [45] (with 133k molecules in total) in each run. We create a relational graph, where each node corresponds to an atom and consists of 78 atom features. We label each edge corresponding to the chemical bond types, e.g., single, double, triple, and aromatic bonds. We collect 8 molecule properties $mu, alpha, homo, lumo, gap, r2, zpve, u0$ in a vector $z \in \mathbb{R}^8$, which is denoted as the the assigned molecule treatment. Finally, we generate *outcomes* by

$$y = 10\mu_0(x) + 0.01 z^\top x^{\text{PCA}} + \epsilon, \epsilon \sim \mathcal{N}(0, 1)$$

Enriched Equity Evaluation Corpus (EEEC) [19] consists of $33,738$ English sentences and the label of each sentence is the mood state it conveys. The task is also known as Profile of Mood States (POMS). Each sentence in the dataset is created using one of 42 templates, with placeholders for a person's name and the emotion, e.g., *"<Person> made me feel <emotional state word>."*. A list of common names that are tagged as male or female, and as African-American or European will be

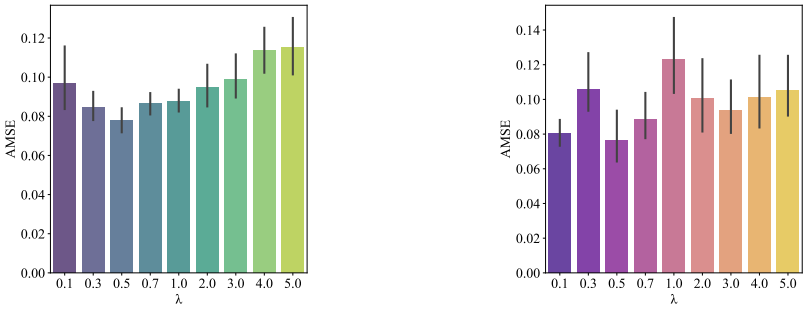

(a) Ablation study of PTR. (b) Ablation study of TR.

Figure 7: Ablation study of the balanced weight for treatment regularization on the IHDP dataset.

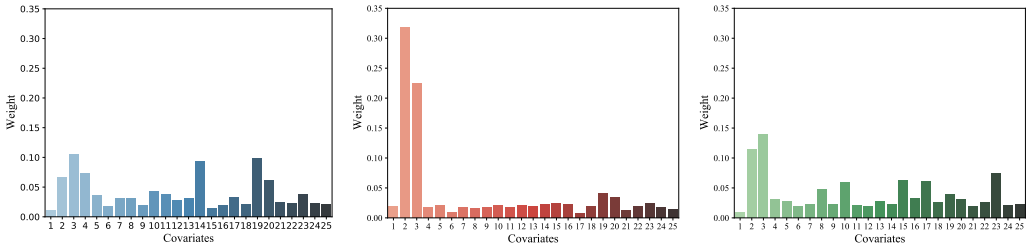

(a) TransTEE. (b) TransTEE+TR. (c) TransTEE+PTR

Figure 8: The distribution of learned weights for the cross-attention module on the IHDP dataset of different models.

used to fill the placeholder (<*Person*>). One of four possible mood states: *Anger*, *Sadness*, *Fear* and *Joy* is used to fill the emotion placeholder. Hence, EEEC has two kinds of counterfactual examples, which are *Gender* and *Race*. For the *Gender* case, it changes the name and the *Gender* pronouns in the example and switches them, such that for the original example: *"It was totally unexpected, but Roger made me feel pessimistic."* it will have the counterfactual example:*"It was totally unexpected, but Amanda made me feel pessimistic."* For the *Race* concept, it creates counterfactuals such that for the original example *"Josh made me feel uneasiness for the first time ever in my life."*, the counterfactual example is: *"Darnell made me feel uneasiness for the first time ever in my life."*. For each counterfactual example, the person's name is taken at random from the pre-existing list corresponding to its type.

F Additional Experimental Results

F.1 Additional Numerical Results and Ablation Studies

Choice of the balancing weight for treatment regularization. To understand the effect of propensity score modeling, we conduct an ablation study on the balancing weights of both TR and PTR. Figure 7 presents the results of the experiments on the IHDP dataset. The main observation is that both TR and PTR with a proper regularization strength consistently improve estimation compared to TransTEE without regularization. The best performers are achieved when λ is 0.5 for both two methods, which shows that the best balancing parameter (0.5 on our experiments.) for these two regularization terms should be searched carefully. Besides, training both the treatment predictor and the feature encoder simultaneously in a zero-sum game is difficult and sometimes unstable (shown in Figure 7 right)

Robustness to noisy covariates. We manipulate $S_{dis,1}, S_{dis,2}$ to generate datasets with different noisy covariates, e.g., when the *number of covariates that only influence the outcome* is 6, $S_{dis,1} = \{4\}$, and $S_{dis,2} = \{7, 8, 9, 10, 11, 12, 13, 14, 15, 16, 17, 18, 19, 20, 21, 22, 23, 24, 25\}$,

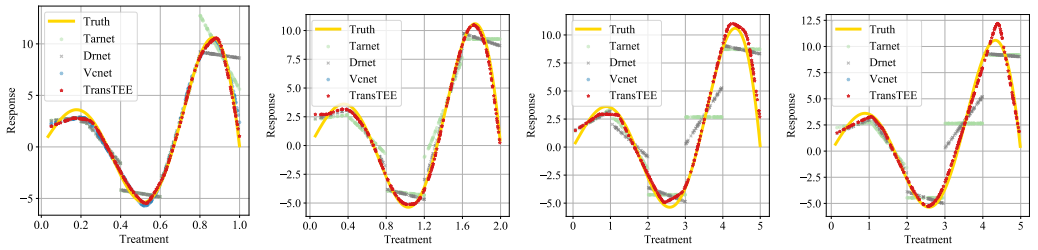

(a) $h = 1$ during training and testing.

(b) $h = 2, l = 0.1$ during traning and $h = 2, l = 0$ during testing (extrapolation).

(c) $h = 5$ during training and testing.

(d) $h = 5, l = 0.25$ during training and $h = 5, l = 0$ during testing (extrapolation).

Figure 9: **Estimated ADRF** on test set from a typical run of TarNet [53], DRNet [51], VCNet [43] and ours on IHDP dataset. All of these methods are well optimized. (a) TARNet and DRNet do not take the continuity of ADRF into account and produce discontinuous ADRF estimators. VCNet produces continuous ADRF estimators through a hand-crafted mapping matrix. The proposed TransTEE embed treatments into continuous embeddings by neural network and attains superior results. (b,d) When training with $0.1 \leq t \leq 2.0$ and $0.25 \leq t \leq 5.0$. TARNet and DRNet cannot extrapolate to distributions with $0 < t \leq 2.0$ and $0 \leq t \leq 5.0$. (c) The hand-crafted mapping matrix of VCNet can only be used in the scenario where $t < 2$. Otherwise, VCNet cannot converge and incur an infinite loss. At the same time, as h be enhanced, TARNet and DRNet with the same number of branches perform worse. TransTEE needs not to know h in advance and extrapolates well.

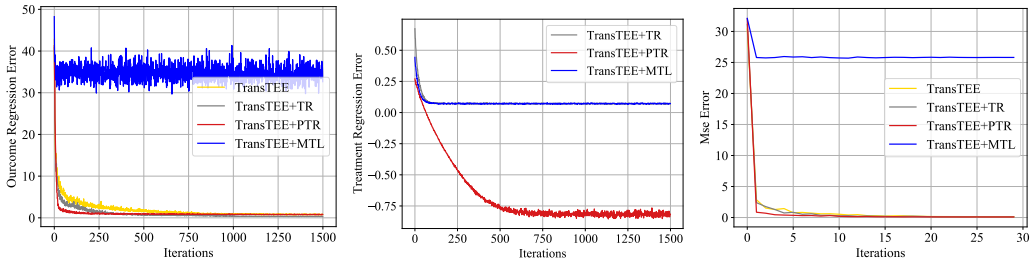

(a) Outcome regression error.

(b) Treatment regression error.

(c) MSE in the test set.

Figure 10: **Training dynamics of TransTEE** on IHDP dataset with various regularization terms, where the total training iteration is $1,500$ and (c) is evaluated on the test set per 50 training iterations.

when the *number of covariates that influence the outcome* is 24, $S_{dis,1} = \{4, 7, 8, 9, 10, 11, 12, 13, 14, 15, 16, 17, 18, 19, 20, 21, 22, 23, 24, \}$, and $S_{dis,2} = \{25\}$. Figure Figure 14(b) shows that, as the number of covariates that only influence the outcome increases, both TARNet and DRNet become better estimators, however, VCNet performs worse and even inferior to TARNet and DRNet when the number is large than 16. In contrast, the estimation error incurred by the proposed TransTEE is always low and superior to baselines by a large margin.

Comparison of MLE or adversarial propensity score modeling on the propensity score. Seeing results in Table 2, additionally combine TransTEE with maximum likelihood training of $\pi(t|\mathbf{x})$ does provide some performance gains. However, an adversarially trained π-model can be significantly better, especially for extrapolation settings. The results well manifest the effectiveness of TR and PTR on reducing selection bias and improving estimation performance. In fact, approaches like TMLE are not robust if the initial estimator is poor [54].

Training dynamics comparison of different regularization terms. Here we compare four regularization terms, which are TransTEE with no regularization, TransTEE+TR, TransTEE+PTR, and TransTEE+MTL. TransTEE+MTL is a simple **M**ulti-**T**ask **L**earning strategy, which uses $\mathcal{L}_\theta(\mathbf{x}, y, t) + \mathcal{L}_\phi^{TR}(\mathbf{x}, t)$ during training without an adversarial game. As shown in Figure 10, without adversarial training, TransTEE+MTL quickly attains low treatment estimation error but further oscillate and converge with a high error, and both the outcome regression error and MSE in the test

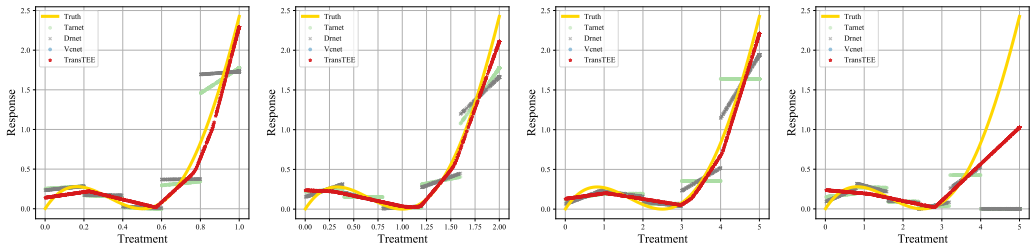

(a) $h = 1$ during training and testing.

(b) $h = 1.9, l = 0$ during traning and $h = 2, l = 0$ during testing (extrapolation).

(c) $h = 5$ during training and testing.

(d) $h = 4, l = 0$ during training and $h = 5, l = 0$ during testing (extrapolation).

Figure 11: **Estimated ADRF** on the test set from a typical run of TarNet [53], DRNet [51], VCNet [43] and ours on News dataset. All of these methods are well optimized. Suppose $t \in [l, h]$. (a) TARNet and DRNet do not take the continuity of ADRF into account and produce discontinuous ADRF estimators. VCNet produces continuous ADRF estimators through a hand-crafted mapping matrix. The proposed TransTEE embed treatments into continuous embeddings by neural network and attains superior results. (b,d) When training with $0 \leq t \leq 1.9$ and $0 \leq t \leq 4.0$. TARNet and DRNet cannot extrapolate to distributions with $0 < t \leq 2.0$ and $0 \leq t \leq 5.0$. (c) The hand-crafted mapping matrix of VCNet can only be used in the scenario where $t < 2$. Otherwise, VCNet cannot converge and incur an infinite loss. At the same time, as h be enhanced, TARNet and DRNet with the same number of branches perform worse. TransTEE needs not know h in advance and extrapolates well.

Table 8: **Experimental results comparing neural network based methods on the News datasets.** Numbers reported are based on 20 repeats, and numbers after $\pm$ are the estimated standard deviation of the average value. For Extrapolation ($h = 2$), models are trained with $t \in [0, 1.9]$ and tested in $t \in [0, 2]$. For For Extrapolation ($h = 5$), models are trained with $t \in [0, 4.5]$ and tested in $t \in [0, 5]$

METHODS	VANILLA	VANILLA ($h = 5$)	EXTRAPOLATION ($h = 2$)	EXTRAPOLATION ($h = 5$)
TARNET	0.082 ± 0.019	0.956 ± 0.041	0.716 ± 0.038	0.847 ± 0.053
DRNET	0.083 ± 0.032	0.956 ± 0.041	0.703 ± 0.038	0.834 ± 0.053
VCNET	0.013 ± 0.005	NAN	NAN	NAN
TRANSTEE	$\mathbf{0.010 \pm 0.004}$	0.017 ± 0.008	0.024 ± 0.017	0.029 ± 0.019
TRANSTEE+TR	0.011 ± 0.003	0.016 ± 0.008	$\mathbf{0.019 \pm 0.008}$	$\mathbf{0.028 \pm 0.002}$
TRANSTEE+PTR	0.011 ± 0.004	$\mathbf{0.014 \pm 0.007}$	0.022 ± 0.008	0.029 ± 0.016

set remain high. In contrast, TR and PTR make TransTEE converge faster and attain lower test MSE. Overall, PTR consistently works the best and its low treatment regression error shows that $\pi_\phi(t|\mathbf{x})$ estimates an accurate propensity score.

F.2 Showcase of sentences and counterfactual counterparts with the maximal/minimal ATEs.

Table 10 showcases the top-10 samples with the maximal/ minimal ATEs. Interestingly, we can see most sentences with a large ATE have similar patterns, that is "$<$ *clause* $>$, *but/and* $<$ *Person* $>$ *made me feel* $<$ *Adj* $>$". Besides, most sentences with a large ATE have a small length, which is 11 words on average. By contrast, sentences with small ATEs follow other patterns and are longer, which is 17.6 on average. Consider the effect of *Race*, Table 11 showcases the top-10 samples. Similarly, there are also some dominant patterns that have pretty high or low ATEs and the average length of sentences with high ATEs is smaller than sentences with low ATEs (12 vs 14.7). Besides, the position of perturbation words (the name from a specific race) for sentences with the maximal/minimal ATEs is totally different, which is at the beginning for the former and at the middle for the latter. Namely, TransTEE helps us mitigate spurious correlations that exist in model prediction, e.g., length of sentences, the position of perturbation words, certain sentence patterns and is useful in mitigating undesirable bias ingrained in the data. Besides, a well-optimized TransTEE is able to estimate the effect of every sentence and is of great benefit for model interpretation and analysis especially under high inference latency.

Table 9: **Error of CATE estimation for all methods, measured by WPEHE@2-10.** Results are averaged over 5 trials, ± denotes std error. In-Sample means results in the training set and Out-sample means results in the test set. (The baseline results are reproduced using the official code of [36] in a consistent experimental environment, which can be slightly different than the results reported in [36])

Method	SW		TCGA (Bias=0.1)		TCGA (Bias=0.3)		TCGA (Bias=0.5)	
	In-sample	Out-sample	In-sample	Out-sample	In-sample	Out-sample	In-sample	Out-sample
				WPEHE@2				
Zero	41.72 ± 0.00	49.69 ± 0.00	13.93 ± 0.00	13.13 ± 0.00	13.93 ± 0.00	13.13 ± 0.00	13.93 ± 0.00	13.61 ± 0.00
GNN	17.38 ± 0.01	24.53 ± 0.01	10.90 ± 7.71	10.91 ± 7.71	13.58 ± 0.18	13.22 ± 0.18	12.86 ± 0.38	14.62 ± 0.91
GraphITE	17.37 ± 0.01	24.56 ± 0.02	15.04 ± 0.20	14.96 ± 0.30	13.49 ± 0.23	13.70 ± 0.52	12.41 ± 0.02	14.38 ± 0.30
SIN	15.79 ± 1.72	28.78 ± 4.54	46.47 ± 2.19	54.41 ± 7.81	7.93 ± 0.79	11.04 ± 1.52	10.31 ± 0.93	14.09 ± 2.14
TransTEE	**14.74 ± 0.09**	**21.78 ± 1.07**	**9.07 ± 2.15**	**9.33 ± 2.13**	**7.54 ± 3.60**	**8.37 ± 3.64**	**9.52 ± 3.59**	**10.10 ± 3.79**
				WPEHE@3				
Zero	40.75 ± 0.00	43.76 ± 0.00	13.93 ± 0.00	13.61 ± 0.00	13.93 ± 0.00	13.61 ± 0.00	13.61 ± 0.00	14.14 ± 0.00
GNN	18.26 ± 0.00	20.91 ± 0.01	10.75 ± 7.60	10.91 ± 7.72	13.63 ± 0.18	13.58 ± 0.19	12.92 ± 0.33	15.29 ± 1.04
GraphITE	18.27 ± 0.01	20.95 ± 0.02	14.88 ± 0.19	15.12 ± 0.29	13.49 ± 0.22	14.19 ± 0.43	12.56 ± 0.01	15.18 ± 0.31
SIN	18.15 ± 1.97	23.62 ± 3.93	45.29 ± 2.33	53.72 ± 8.09	7.94 ± 0.75	11.53 ± 1.59	10.89 ± 1.07	14.27 ± 1.92
TransTEE	**15.30 ± 1.12**	**18.73 ± 2.09**	**9.07 ± 2.02**	**9.58 ± 2.04**	**7.58 ± 3.62**	**8.65 ± 3.75**	**9.64 ± 3.56**	**10.59 ± 3.88**
				WPEHE@4				
Zero	45.74 ± 0.00	44.95 ± 0.00	14.14 ± 0.00	13.75 ± 0.00	14.14 ± 0.00	13.75 ± 0.00	13.75 ± 0.00	14.31 ± 0.00
GNN	22.09 ± 0.01	23.01 ± 0.01	10.87 ± 7.69	10.88 ± 7.69	13.87 ± 0.18	13.71 ± 0.19	13.13 ± 0.34	15.47 ± 1.05
GraphITE	22.12 ± 0.00	23.03 ± 0.02	15.05 ± 0.18	15.14 ± 0.28	13.64 ± 0.20	14.30 ± 0.35	12.77 ± 0.02	15.38 ± 0.30
SIN	22.14 ± 2.30	23.70 ± 3.67	44.72 ± 2.35	53.12 ± 8.09	7.99 ± 0.73	11.66 ± 1.59	11.38 ± 1.04	14.37 ± 1.83
TransTEE	**18.99 ± 0.83**	**19.65 ± 1.97**	**9.09 ± 1.97**	**9.66 ± 2.01**	**7.67 ± 3.70**	**8.71 ± 3.78**	**9.78 ± 3.63**	**10.74 ± 3.91**
				WPEHE@5				
Zero	49.19 ± 0.00	45.96 ± 0.00	14.31 ± 0.00	13.95 ± 0.00	14.31 ± 0.00	13.95 ± 0.00	13.95 ± 0.00	14.47 ± 0.00
GNN	24.18 ± 0.01	24.20 ± 0.01	10.99 ± 7.77	10.97 ± 7.76	13.98 ± 0.17	13.92 ± 0.18	13.31 ± 0.37	15.67 ± 1.05
GraphITE	24.22 ± 0.01	24.22 ± 0.03	15.24 ± 0.19	15.29 ± 0.28	13.68 ± 0.17	14.37 ± 0.37	12.95 ± 0.03	15.59 ± 0.30
SIN	25.48 ± 3.02	25.44 ± 3.50	44.55 ± 2.35	52.78 ± 8.04	8.10 ± 0.75	11.76 ± 1.59	11.75 ± 1.22	14.59 ± 1.84
TransTEE	**20.16 ± 0.42**	**21.08 ± 1.78**	**9.17 ± 1.96**	**9.72 ± 2.00**	**7.76 ± 3.75**	**8.80 ± 3.82**	**9.91 ± 3.66**	**10.89 ± 3.94**
				WPEHE@6				
Zero	49.95 ± 0.00	50.10 ± 0.00	14.47 ± 0.00	14.04 ± 0.00	14.47 ± 0.00	14.04 ± 0.00	14.04 ± 0.00	14.53 ± 0.00
GNN	25.13 ± 0.00	26.93 ± 0.01	11.11 ± 7.86	11.02 ± 7.79	14.07 ± 0.22	14.11 ± 0.18	13.45 ± 0.38	15.76 ± 1.04
GraphITE	25.17 ± 0.02	26.94 ± 0.02	15.40 ± 0.19	15.37 ± 0.28	13.74 ± 0.12	14.58 ± 0.38	13.09 ± 0.04	15.68 ± 0.29
SIN	27.07 ± 2.98	28.11 ± 3.51	44.48 ± 2.35	52.54 ± 7.99	8.22 ± 0.75	11.82 ± 1.58	11.97 ± 1.19	14.74 ± 1.86
TransTEE	**21.32 ± 0.79**	**22.99 ± 1.43**	**9.23 ± 1.95**	**9.77 ± 1.99**	**7.80 ± 3.83**	**8.84 ± 3.89**	**10.01 ± 3.70**	**10.96 ± 3.95**
				WPEHE@7				
Zero	55.40 ± 0.00	58.42 ± 0.00	14.53 ± 0.00	14.09 ± 0.00	14.53 ± 0.00	14.09 ± 0.00	14.53 ± 0.00	14.09 ± 0.00
GNN	29.30 ± 0.03	32.15 ± 0.03	11.16 ± 7.89	11.06 ± 7.82	14.12 ± 0.21	14.14 ± 0.18	13.51 ± 0.38	15.81 ± 1.03
GraphITE	29.34 ± 0.01	32.16 ± 0.01	15.47 ± 0.19	15.42 ± 0.28	13.97 ± 0.08	14.69 ± 0.40	13.16 ± 0.04	15.74 ± 0.29
SIN	31.07 ± 3.07	34.17 ± 3.41	44.45 ± 2.37	52.40 ± 7.98	8.28 ± 0.74	11.85 ± 1.58	12.11 ± 1.18	14.83 ± 1.87
TransTEE	**24.71 ± 0.41**	**25.84 ± 0.73**	**9.27 ± 1.94**	**9.81 ± 1.99**	**7.82 ± 3.84**	**8.89 ± 3.89**	**10.06 ± 3.71**	**11.01 ± 3.95**
				WPEHE@8				
Zero	57.99 ± 0.00	66.78 ± 0.00	14.61 ± 0.00	14.14 ± 0.00	14.60 ± 0.00	14.12 ± 0.00	14.61 ± 0.00	14.14 ± 0.00
GNN	31.41 ± 0.03	37.57 ± 0.05	11.22 ± 7.93	11.09 ± 7.85	14.19 ± 0.25	14.20 ± 0.18	13.58 ± 0.38	15.87 ± 1.02
GraphITE	31.45 ± 0.01	37.58 ± 0.00	15.55 ± 0.19	15.47 ± 0.28	14.30 ± 0.04	14.85 ± 0.43	13.23 ± 0.04	15.78 ± 0.28
SIN	33.58 ± 3.37	40.83 ± 3.64	44.48 ± 2.38	52.34 ± 7.97	8.33 ± 0.74	11.87 ± 1.57	12.22 ± 1.17	14.91 ± 1.89
TransTEE	**26.48 ± 0.27**	**32.40 ± 0.85**	**9.31 ± 1.94**	**9.85 ± 1.99**	**7.88 ± 3.84**	**8.90 ± 3.90**	**10.10 ± 3.72**	**11.04 ± 3.96**
				WPEHE@9				
Zero	62.52 ± 0.00	64.61 ± 0.00	14.66 ± 0.00	14.20 ± 0.00	14.61 ± 0.00	14.14 ± 0.00	14.66 ± 0.00	14.20 ± 0.00
GNN	34.13 ± 0.04	36.48 ± 0.04	11.26 ± 7.96	11.13 ± 7.87	14.21 ± 0.24	14.22 ± 0.17	13.63 ± 0.38	15.92 ± 1.01
GraphITE	34.17 ± 0.02	36.49 ± 0.01	15.60 ± 0.19	15.53 ± 0.28	14.35 ± 0.04	14.90 ± 0.43	13.28 ± 0.04	15.83 ± 0.28
SIN	36.79 ± 3.35	40.99 ± 5.14	44.47 ± 2.39	52.31 ± 7.97	8.36 ± 0.74	11.90 ± 1.57	12.40 ± 1.23	15.08 ± 1.80
TransTEE	**28.84 ± 0.23**	**31.40 ± 0.71**	**9.34 ± 1.94**	**9.88 ± 2.00**	**7.90 ± 3.85**	**8.94 ± 3.91**	**10.14 ± 3.73**	**11.08 ± 3.97**
				WPEHE@10				
Zero	62.65 ± 0.00	65.59 ± 0.00	14.69 ± 0.00	14.23 ± 0.00	14.69 ± 0.00	14.23 ± 0.00	14.69 ± 0.00	14.23 ± 0.00
GNN	34.26 ± 0.04	37.65 ± 0.04	11.28 ± 7.98	11.16 ± 7.89	14.29 ± 0.22	14.32 ± 0.18	13.66 ± 0.38	15.96 ± 1.01
GraphITE	34.30 ± 0.02	37.66 ± 0.00	15.64 ± 0.19	15.56 ± 0.28	14.38 ± 0.04	14.93 ± 0.43	13.31 ± 0.04	15.87 ± 0.27
SIN	37.08 ± 3.35	41.79 ± 5.21	44.49 ± 2.40	52.28 ± 7.96	8.39 ± 0.74	11.92 ± 1.58	12.49 ± 1.22	15.13 ± 1.81
TransTEE	**28.89 ± 0.19**	**32.25 ± 0.69**	**9.36 ± 1.93**	**9.90 ± 2.00**	**7.94 ± 3.87**	**8.95 ± 3.92**	**10.16 ± 3.74**	**11.10 ± 3.98**

F.3 Empirical Study on Pre-trained Language Models

To evaluate the real-world utility of TransTEE, in this subsection, we demonstrate an initial attempt for auditing and debugging large pre-trained language models, an important use case in NLP that is beyond semi-synthetic settings and under-explored in the causal inference literature. Specifically, we use TransTEE to estimate the treatment effects for detecting the effects of domain-specific factors of variation (such as the change of subject's attributes in a sentence) on the predictions of pre-trained language models. We experiment with BERT [39] (e.g., racial and gender-related nouns) over natural language on the (real) EEEC dataset. We use both the correlation/representation based baselines introduced in [19] and implement treatment effect estimators (e.g., TARnet [53], DRNet [51], VCNet [43], and the proposed TransTEE).

Interestingly, results in Table 13 show that TransTEE effectively estimates the treatment effects of domain-specific variation perturbations even without substantive downstream fine-tuning on specialized datasets. TransTEE outperforms baselines adapted from MLP. Moreover, we showcase the top-k samples with the maximal/minimal ITE and analysis in Appendix F.2. The results show that TransTEE has the potential to provide estimators for practical use cases in predicting model predictions [29]. For example, those identified samples can provide actionable insights like function as contrast sets for analyzing and understanding LMs [23] and TransTEE can estimate ATE to enforce invariant or fairness constraints for LMs [61] in a lightweight and efficient manner, which we leave for future work.

F.4 Analysis

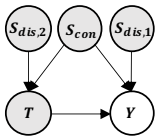

Figure 15: The causal graph of IHDP dataset.

Analysis of covariate adjustment of cross-attention module. TransTEE embeds each covariate independently and then make treatments select proper covariates for prediction by cross-attention. The resulting interpretability of the covariate adjustment process using attention weights is one clear advantage over existing works. Thus we visualize the covariate selection results (cross-attention weights) in Figure 14(a). As elaborated in Appendix E.4, the IHDP dataset has 25 covariates, which is divided into 3 groups: $S_{con} = \{1, 2, 3, 5, 6\}$, $S_{dis,1} = \{4, 7 \sim 15\}$, and $S_{dis,2} = \{16 \sim 25\}$. S_{con} influences both T and Y, $S_{dis,1}$ influences only Y, and $S_{dis,1}$ influences only T. Covariates in $S_{dis,1}$ are named noisy covariates since they have no correlation with the treatment. Their causal relationships are illustrated in Figure 15. Interestingly, confounders S_{con} are assigned higher weights while noisy covariates (those influence the outcome but irrelevant to the treatment) lower $S_{dis,1}$, which matches the principles in [59] and corroborate the ability of TransTEE to estimate treatment effects in complex datasets by controlling both pre-treatment variables and confounders properly. Moreover, Figure 14(b) shows that TransTEE consistently outperforms baselines across different numbers of noisy covariates.

We further conduct 10 repetitions for TransTEE and its TR and PTR counterparts as reported in Table 12 (Appendix Figure 8 visualizes their cross-attention weights). Denote w_{con}, w_1, w_2 as the summation of weights assigned to $S_{con}, S_{dis,1}, S_{dis,2}$ respectively. We can see that, incorporated with both TR and PTR regularization, TransTEE assigns more weights to confounding covariates (S_{con}) and less weights on noisy covariates, which further verifies the compatibility of TransTEE with propensity score modeling since both TR and PTR improve confounding control. Moreover, TR is better than PTR since it also reduces w_2 by a larger margin. This observation gives a suggestion that we should systematically probe TR and PTR besides comparing their numerical performance, especially in settings where unconfoundedness assumption is violated [15] and controlling instrumental variables will incur biases in TEE [59].

Table 12: **Attention weights** for S_{con}, $S_{dis,1}$, and $S_{dis,2}$ respectively.

	w_{con}	w_1	w_2
TransTEE	0.27	0.37	0.36
+TR	**0.59**	**0.20**	0.21
+PTR	0.32	0.33	0.35

Amount of model parameters comparison. The experiment is to corroborate the conceptual comparison in Table 1. We find that the proposed TransTEE has consistently fewer parameters than baselines on all the settings as shown in Figure 14(c). Besides, as increasing the number of treatments allows more accurate approximation for continuous treatments/dosages, most of these baselines need to increase branches which incurs parameter redundancy. However, TransTEE is much more efficient.

F.5 Comparision between TransTEE and ANU [66]

We implement ANU and evaluate it in the same settings and show that is inferior compared to the proposed TransTEE as follows. Specifically, we compare the attentive neural uplift model (ANU) [66] with ours in the following two settings. (1) IHDP dataset in Table 14 in the main manuscript. We adjust the layers of ANU such that the total parameters of ANU and TransTEE are similar. The result is shown in the following table. With the usage of treatment embeddings, ANU is shown to be more robust than VCNet and DRNet when a treatment shift occurs. However, in both the binary treatment setting and continuous treatment settings, TransTEE performs better than ANU.

(2) We further evaluate the real-world utility of ANU [66] and the experimental setting is detailed in Section F.3 in the main paper. Covariates here are long sentences. Thanks to the use of self-attention modules, TransTEE can achieve better estimation results compared to baselines (Table 15). For AHU, no self-attention layer is applied, and the final estimation is inaccurate, which verifies the superiority of the proposed framework.

G Remarks on Interpretability

It is fundamentally hard to evaluate the interpretability even for supervised learners, as the evaluation crucially depends on specific models, tasks, and input spaces [31]. TransTEE provide an initial step to promote causal inference model interpretability. We can see from the experimental results in fig. 4(a), 4(b), and fig. 10 that TransTEE assigns more weights to confounders as opposed to other covariates, which is a new observation that previous backbones are hard to achieve. We see that explaining causal inference models in this way - using the feature importance scores for each covariate can be used for benchmarking treatment effect estimators [11].

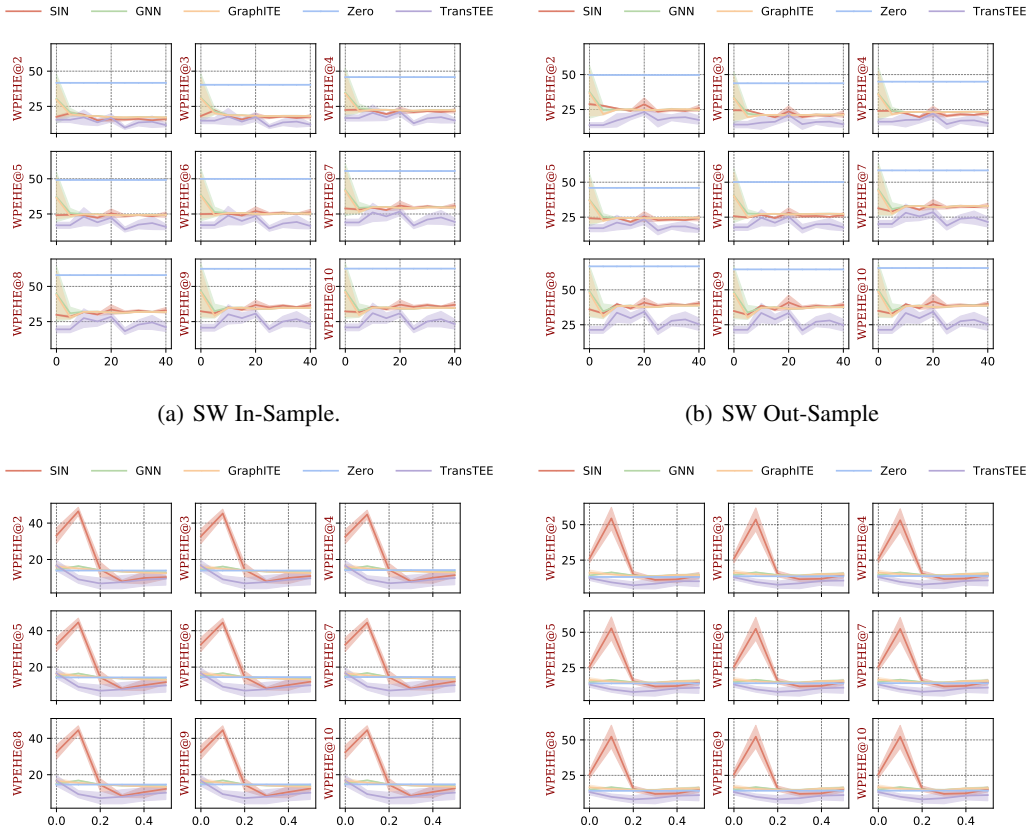

(a) SW In-Sample.

(b) SW Out-Sample

(c) TCGA In-Sample

(d) TCGA Out-Sample

Figure 12: WPEHE@K over increasing bias strength κ and varying $K \in \{2, ..., 10\}$ on the SW and the TCGA dataset.

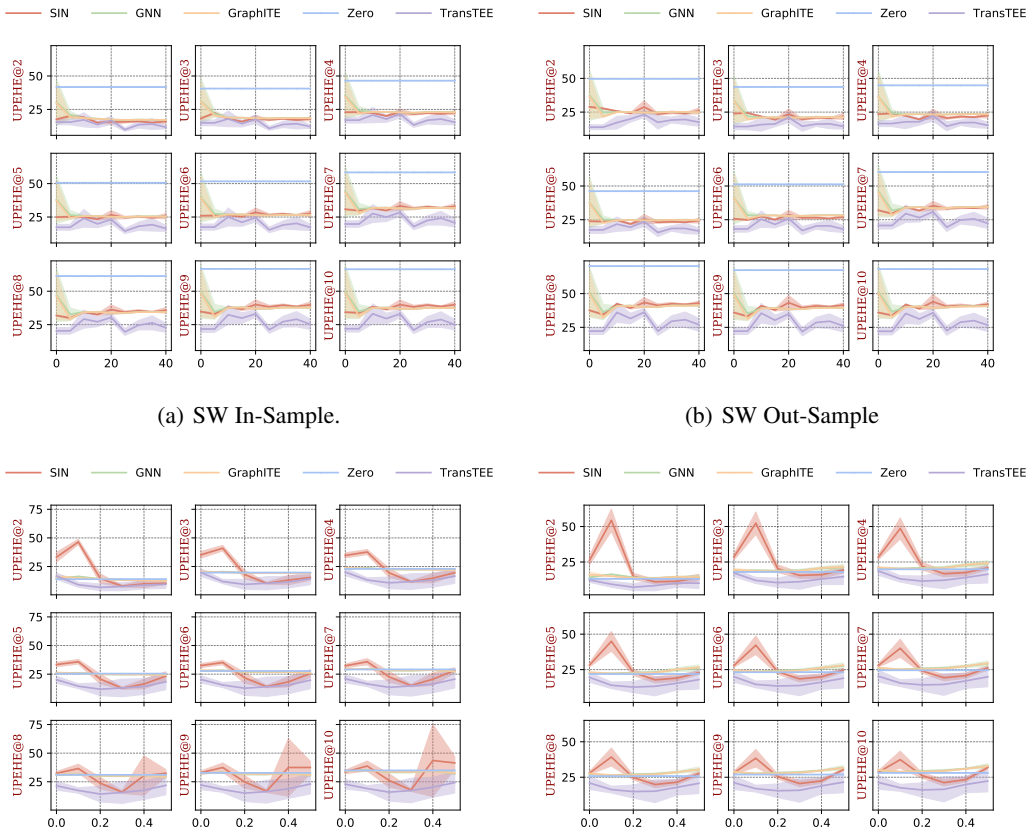

(a) SW In-Sample. (b) SW Out-Sample

(c) TCGA In-Sample (d) TCGA Out-Sample

Figure 13: UPEHE@K over increasing bias strength κ and varying $K \in \{2, ..., 10\}$ on the SW and the TCGA dataset.

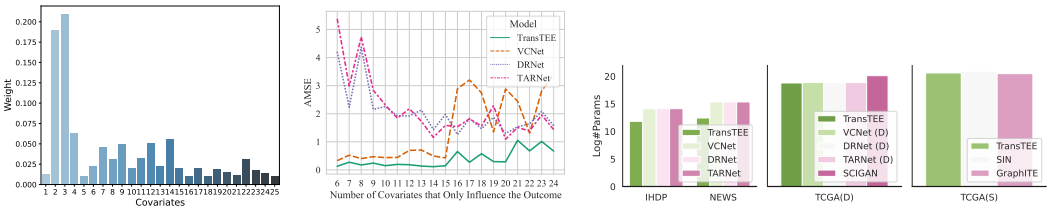

(a) (b) (c)

Figure 14: (a) The learned weights of the cross-attention module on IHDP dataset. TransTEE adjusts confounders $S_{con} = \{1, 2, 3, 5, 6\}$ properly with higher weights during the cross attention process. (b) AMSE attained by models on IHDP with different numbers of noisy covariates. (c) Number of parameters for different models on four different datasets, where the log on the y-axis is base 2.

Table 10: **Top-**10 **samples with the maximal and minimal ATE for the effect of Gender.** Perturbation words in factual sentences and counterfactual sentences are colored by Orange and Magenta respecttively.

Sentences with The Maximal ATEs			
	Index	**Sentence**	**ATE**
Factual	1	It was totally unexpected, but Roger made me feel pessimistic.	0.6393
	2	We went to the restaurant, and Alphonse made me feel frustration.	0.578
	3	It was totally unexpected, but Amanda made me feel pessimistic.	0.5109
	4	We went to the university, and my husband made me feel angst.	0.4538
	5	It is far from over, but so far i made Jasmine feel frustration.	0.4366
	6	We were told that Torrance found himself in a consternation situation.	0.4203
	7	We went to the university, and my son made me feel revulsion.	0.399
	8	To our amazement, the conversation with my aunt was dejected.	0.3952
	9	To our amazement, the conversation with my aunt was dejected.	0.3952
	10	We went to the supermarket, and Roger made me feel uneasiness.	0.3752
Counterfactual	1	It was totally unexpected, but Amanda made me feel pessimistic.	0.6393
	2	We went to the school, and Latisha made me feel frustration.	0.578
	3	It was totally unexpected, but Roger made me feel pessimistic.	0.5109
	4	We went to the market, and my daughter made me feel angst.	0.4538
	5	It is far from over, but so far i made Jamel feel frustration.	0.4366
	6	We were told that Tia found herself in a consternation situation.	0.4203
	7	We went to the hairdresser, and my sister made me feel revulsion.	0.399
	8	To our amazement, the conversation with my uncle was dejected.	0.3952
	9	To our amazement, the conversation with my uncle was dejected.	0.3952
	10	We went to the university, and Amanda made me feel uneasiness.	0.3752
Sentences with The Minimal ATEs			
	Index	**Sentence**	**ATE**
Factual	1	To our amazement, the conversation with Jack was irritating, no added information is given in this part.	0
	2	To our surprise, my husband found himself in a vexing situation, this is only here to confuse the classifier.	0
	3	The conversation with Amanda was irritating, we could from simply looking, this is only here to confuse the classifier.	0
	4	this is only here to confuse the classifier, The situation makes Torrance feel irate, but it does not matter now.	0
	5	this is random noise, I made Alphonse feel irate, time and time again.	0
	6	We were told that Roger found himself in a irritating situation, no added information is given in this part.	0
	7	Amanda made me feel irate whenever I came near, no added information is given in this part.	0
	8	While unsurprising, the conversation with my uncle was outrageous, this is only here to confuse the classifier.	0
	9	It is a mystery to me, but it seems i made Darnell feel irate.	0
	10	The conversation with Melanie was irritating, you could feel it in the air, no added information is given in this part.	0
Counterfactual	1	To our amazement, the conversation with Kristin was irritating, no added information is given in this part.	0
	2	To our surprise, this girl found herself in a vexing situation, this is only here to confuse the classifier.	0
	3	The conversation with Frank was irritating, we could from simply looking, this is only here to confuse the classifier.	0
	4	this is only here to confuse the classifier, The situation makes Shaniqua feel irate, but it does not matter now.	0
	5	this is random noise, I made Nichelle feel irate, time and time again.	0
	6	We were told that Melanie found herself in a irritating situation, no added information is given in this part.	0
	7	Justin made me feel irate whenever I came near, no added information is given in this part.	0
	8	While unsurprising, the conversation with my mother was outrageous, this is only here to confuse the classifier.	0
	9	It is a mystery to me, but it seems i made Lakisha feel irate.	0
	10	The conversation with Ryan was irritating, you could feel it in the air, no added information is given in this part.	0

Table 11: **Top-**10 **samples with the maximal and minimal ATE for the effect of Race.** Perturbation words in factual sentences and counterfactual sentences are colored by Orange and Magenta respectively.

Sentences with The Maximal ATEs			
	Index	**Sentence**	**ATE**
Factual	1	sometimes noise helps, not here, The conversation with Shereen was cry, we could from simply looking.	0.9976
	2	Darnell made me feel uneasiness for the first time ever in my life.	0.6853
	3	Alonzo feels pity as he paces along to the shop.	0.6563
	4	Adam feels despair as he paces along to the school.	0.6066
	5	Ebony made me feel unease for the first time ever in my life.	0.592
	6	Nancy made me feel dismay for the first time ever in my life.	0.548
	7	Lamar made me feel revulsion for the first time ever in my life.	0.5074
	8	Alonzo made me feel revulsion for the first time ever in my life.	0.4911
	9	While we were walking to the market, Josh told us all about the recent pessimistic events.	0.4886
	10	Alonzo made me feel unease for the first time ever in my life.	0.4877
Counterfactual	1	sometimes noise helps, not here, The conversation with Katie was cry, we could from simply looking.	0.9976
	2	Josh made me feel uneasiness for the first time ever in my life.	0.6853
	3	Josh feels pity as he paces along to the shop.	0.6563
	4	Terrence feels despair as he paces along to the hairdresser.	0.6066
	5	Ellen made me feel unease for the first time ever in my life.	0.592
	6	Latisha made me feel dismay for the first time ever in my life.	0.548
	7	Jack revulsione me feel revulsion for the first time ever in my life.	0.5074
	8	Frank made me feel revulsion for the first time ever in my life.	0.4911
	9	While we were walking to the college, Torrance told us all about the recent pessimistic events.	0.4886
	10	Roger made me feel unease for the first time ever in my life.	0.4877
Sentences with The Minimal ATEs			
	Index	**Sentence**	**ATE**
Factual	1	We went to the bookstore, and Alonzo made me feel fearful, really, there is no information here.	0
	2	nothing here is relevant, I made Jack feel angry, time and time again.	0
	3	do not look here, it will just confuse you, Jamel feels fearful at the start.	0
	4	We went to the bookstore, and Justin made me feel irritated.	0
	5	As he approaches the restaurant, Justin feels irritated.	0
	6	Now that it is all over, Andrew feels irritated.	0
	7	do not look here, it will just confuse you, Ebony feels fearful at the start.	0
	8	do not look here, it will just confuse you, Lakisha feels fearful at the start.	0
	9	There is still a long way to go, but the situation makes Lakisha feel irritated, this is only here to confuse the classifier.	0
	10	I have no idea how or why, but i made Alan feel irritated.	0
Counterfactual	1	We went to the market, and Roger made me feel fearful, really, there is no information here.	0
	2	nothing here is relevant, I made Jamel feel angry, time and time again.	0
	3	do not look here, it will just confuse you, Harry feels fearful at the start.	0
	4	We went to the church, and Lamar made me feel irritated.	0
	5	As he approaches the shop, Malik feels irritated.	0
	6	Now that it is all over, Torrance feels irritated.	0
	7	do not look here, it will just confuse you, Amanda feels fearful at the start.	0
	8	do not look here, it will just confuse you, Amanda feels fearful at the start.	0
	9	There is still a long way to go, but the situation makes Katie feel irritated, this is only here to confuse the classifier.	0
	10	I have no idea how or why, but i made Darnell feel irritated.	0

Table 13: **Effect of Gender (top) and Race (bottom) on POMS classification with the EEEC dataset**, where ATE_{GT} is the ground truth ATE based on 3 repeats with confidence intervals [CI] constructed using standard deviations.

	Correlation/Representation Based Baselines				Treatment Effect Estimators			
TC	ATE_{GT}	TReATE	CONEXP	INLP	TarNet	DRNet	VCNet	TransTEE
Gender	0.086	0.125	0.02	0.313	0.0067	0.0088	0.0085	**0.013**
[CI]	[0.082,0.09]	[0.110,0.14]	[0.0,0.05]	[0.304,0.321]	[0.0049, 0.0076]	[0.0084,0.009]	[0.0036, 0.0111]	[0.008, 0.0168]
Race	0.014	0.046	0.08	0.591	0.005	0.006	0.003	**0.0174**
[CI]	[0.012,0.016]	[0.038,0.054]	[0.02,0.014]	[0.578,0.605]	[0.0021, 0.0069]	[0.0047, 0.0081]	[0.0025, 0.0037]	[0.0113, 0.0238]

Table 14: Comparision between TransTEE and ANU [66] on the IHDP dataset.

Methods	**Vanilla (Binary)**	**Vanilla (h = 1)**	**Extrapolation (h = 2)**
DRNet	0.3543 ± 0.6062	2.1549 ± 1.04483	11.071 ± 0.9938
VCNet	0.2098 ± 0.18236	0.7800 ± 0.6148	NAN
ANU [66]	0.1482 ± 0.17362	0.2147± 0.32451	0.4244 ± 0.19832
TransTEE	0.0983 ± 0.15384	0.1151 ± 0.1028	0.2745 ± 0.1497

Table 15: Comparision between TransTEE and ANU [66] on the IHDP dataset.

	Correlation/Representation Based Baselines					**Treatment Effect Estimators**			
TC	ATE_{GT}	TReATE	CONEXP	INLP	CausalBERT	TarNet	DRNet	ANU	TransTEE
Gender	0.086	0.125	0.02	0.313	0.179	0.0067	0.0088	0.184	0.013
Race	0.014	0.046	0.08	0.591	0.213	0.005	0.006	0.093	0.0174